

# Tazza: Shuffling Neural Network Parameters for Secure and Private Federated Learning

KICHANG LEE, Yonsei University, Republic of Korea

JAEHO JIN, Yonsei University, Republic of Korea

JAEYEON PARK, Dankook University, Republic of Korea

SONGKUK KIM, Yonsei University, Republic of Korea

JEONGGIL KO, Yonsei University, POSTECH, Republic of Korea

Federated learning is an innovative computing paradigm that enables decentralized model training without sharing raw data from individual user/client devices, thereby preserving their data privacy. However, federated learning systems still face significant security challenges, from attacks including data leakage via gradient inversion and model poisoning from malicious clients. Existing solutions often address these issues in isolation, which compromises either system robustness or model accuracy. In this paper, we present *Tazza*, a secure and efficient federated learning framework designed to tackle both challenges simultaneously. By leveraging the permutation equivariance and invariance property inherent in modern neural network architectures, *Tazza* enhances resilience against diverse poisoning attacks, including noise injection and backdoor attacks, while ensuring data confidentiality and maintaining high model accuracy. Evaluations using various datasets and embedded computing platforms show that *Tazza* achieves robust defense with up to  $6.7\times$  improved computational efficiency compared to alternative schemes, without compromising the federated learning model performance.

## 1 INTRODUCTION

Federated learning is a transformative paradigm that facilitates training machine learning models in decentralized environments while preserving the privacy of data stored on distributed mobile and embedded devices [38] and enhancing personalized user experiences in ubiquitous computing applications. In federated learning, clients perform local model training over several epochs and share model updates, rather than raw data, with a central server. The server then aggregates these updates across clients over multiple rounds, collaboratively building a robust global model. This decentralized approach is particularly promising for mobile and embedded computing systems [2, 56], given that it enables them to leverage vast amounts of (distributed) locally collected data for maintaining a high-performing personalized model while alleviating many of the privacy and network overhead concerns that arise from sharing personal data/information [55].

However, despite its decentralized and privacy-preserving nature stemming from the fact that local information of individual users/devices is not shared directly with the server, federated learning still faces significant privacy and security threats. Unlike centralized training, where data resides on a single server, federated learning relies on distributed, heterogeneous user/client data, leaving it vulnerable to malicious model updates that compromise system integrity [19, 21]. Furthermore, honest-but-curious servers can attempt to analyze model updates to infer private user data, breaching confidentiality [18, 22]. These concerns are particularly critical in ubiquitous computing scenarios, such as daily activity and personal health monitoring, where sensitive data is abundant, and the software environment is vulnerable due to the ease of installing third-party apps [33, 34]. These threats are categorized into two primary attack vectors: **integrity attacks**, in which malicious clients undermine model robustness, and **confidentiality attacks**, where curious servers endanger data privacy.

Specifically, integrity attacks involve malicious clients disrupting federated learning by sharing tampered updates, such as injecting noise [21], training with incorrect labels [6, 24], or embedding adversarial patterns [4].

---

Authors' addresses: Kichang Lee, kichang.lee@yonsei.ac.kr, Yonsei University, Republic of Korea; Jaeho Jin, jaeho.jin.eis@yonsei.ac.kr, Yonsei University, Republic of Korea; JaeYeon Park, jaeyeon.park@dankook.ac.kr, Dankook University, Republic of Korea; Songkuk Kim, songkuk@yonsei.ac.kr, Yonsei University, Republic of Korea; JeongGil Ko, jeonggil.ko@yonsei.ac.kr, Yonsei University, POSTECH, Republic of Korea.

Without effective defense, these integrity attacks hinder global model convergence and performance. Existing solutions include filtering tampered updates using statistical priors [65] or employing robust aggregation [7, 9]. Furthermore, confidentiality attacks, where the server aims to infer client data from model updates, are typically countered by techniques like differential privacy [1, 17] or gradient pruning [70]. However, such methods often compromise global model convergence due to altered updates [27]. This paper aims to comprehensively address these challenges.

We emphasize that ensuring both **integrity** and **confidentiality** is critical in federated learning, particularly for mobile and embedded systems. With large-scale participation from distributed and often anonymous clients, it is unrealistic to assume that all participants act in good faith. Robust mechanisms are needed to defend against malicious clients that compromise the integrity of the system. Equally important is safeguarding sensitive data collected from mobile and embedded devices, such as health information [45, 47], daily activities [23, 46, 66], or environmental metrics [58, 63] to maintain user trust and meet privacy regulations.

However, simultaneously addressing integrity and confidentiality presents unique challenges. Traditional confidentiality measures, such as noise addition, protect privacy by obscuring model updates but can inadvertently impede the detection of malicious patterns, including backdoor attacks or label poisoning. On the other hand, integrity defenses aim to identify and mitigate these threats but may conflict with confidentiality measures, complicating the design of robust systems that achieve both objectives. This complexity is further amplified by the non-i.i.d. nature of real-world data, where the diversity of benign model updates makes it challenging to distinguish legitimate updates from malicious ones, especially when inaccuracies are introduced by confidentiality defenses. These trade-offs create significant barriers to ensuring security and privacy without compromising global model performance.

Despite the critical importance of these issues, not many previous works target to simultaneously address integrity and confidentiality threats while preserving model performance. Nevertheless, tackling this intertwined challenge is imperative for real-world federated learning applications, where system reliability and user trust depend on effective, balanced defense mechanisms.

In this paper, we address the challenges of ensuring both integrity and confidentiality in federated learning by leveraging the permutation equivariant and invariant properties of neural networks (c.f., Sec 2.2). Permutation equivariance ensures that a function’s output changes consistently with the order of its inputs, while permutation invariance guarantees the output remains unchanged regardless of input order. These properties are fundamental to widely used neural network architectures, including multilayer perceptrons (MLPs), recurrent neural networks (RNNs), and Transformers.

Leveraging these properties, we propose *Tazza*, a novel framework that ensures both confidentiality and integrity in federated learning. Specifically, *Tazza* implements a weight shuffling module that rearranges neural network parameters according to a predefined shuffling rule, effectively obscuring sensitive information. This shuffling process is designed to be computationally efficient, making it suitable for deployment on mobile and embedded devices. Additionally, *Tazza* includes a shuffled model validation process, which verifies the integrity of the shuffled models by ensuring consistent outputs, thereby maintaining model performance in ubiquitous computing scenarios.

Nevertheless, properly shuffling model parameters while preserving the desired properties is a challenging task, as it requires a deep understanding of the intricate operations within neural networks. Moreover, while many network architectures exhibit permutation equivariant and invariant properties, the underlying mechanisms that enable these properties vary significantly across different models. For this, we introduce tailored algorithms for representative neural network architectures, providing a systematic approach to better understand and exploit these properties. Using our insights and experience, we demonstrate how these algorithms can effectively harness permutation-based properties, paving the way for practical applications in federated learning.

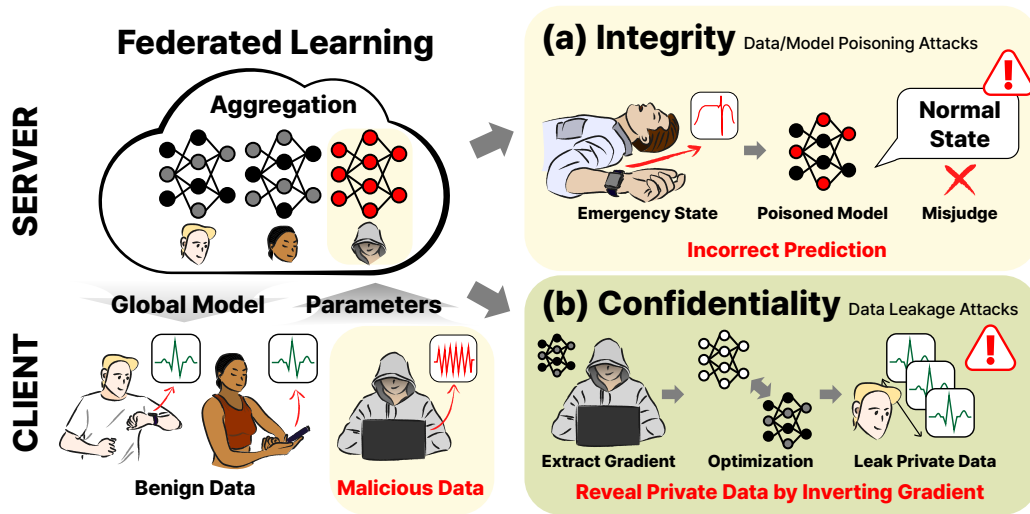


Fig. 1. Integrity and confidentiality attack threats in a federated learning scenario.

To implement the aforementioned properties, *Tazza* employs a novel weight shuffling module, designed to (intentionally) obscure the original model by rearranging its weights while maintaining permutation equivariant and invariant properties. The operations of this module ensure that the shuffled model remains valid, which is maintained by a shuffled validation process for integrity checks, confirming that model outputs remain accurate despite weight shuffling. Finally, we leverage the similarity metrics obtained from the shuffled validation process and cluster the models to distinguish and isolate malicious updates from impacting benign models.

By integrating these components, we present *Tazza* as a secure, privacy-preserving, and accurate federated learning framework that effectively addresses both integrity and confidentiality challenges, thereby fostering trust and facilitating broader ubiquitous computing among users of mobile and embedded devices. Along with a strong mathematical foundation leveraging permutation properties, we demonstrate its practical efficacy through extensive evaluations on diverse datasets and embedded platforms. Specifically, *Tazza* maintains high model accuracy while mitigating both integrity and confidentiality attacks, with a computational speedup of up to 6.7 $\times$  compared to alternative defense schemes. Our key contributions are summarized as follows:

- Building on mathematical evidence, we propose an effective and efficient model-securing mechanism tailored for federated learning scenarios. This mechanism leverages the permutation equivariance and invariance properties of neural networks through two key components: *Weight Shuffling* and *Shuffled Model Validation*.
- By seamlessly integrating Weight Shuffling and Shuffled Validation, we present *Tazza*, a privacy-preserving and secure federated learning framework specifically designed for mobile and embedded scenarios, achieving robust security without compromising model performance.
- We conduct an extensive evaluation of *Tazza* across diverse datasets, model architectures, and attack scenarios. Our results demonstrate that *Tazza* effectively isolates malicious model updates from benign ones to counter integrity attacks, while its model parameter shuffling mechanism robustly mitigates confidentiality attacks.

	Confidentiality	Integrity	Performance w/o Integration	Performance w/ Integration	On-device Computation	Core Features
FedAvg [38]	✗	✗	✓	✗	↓	No defense mechanism
Median [64]	✗	⚠	⚠	✗	↓	Statistical Prior (Median Aggregation)
Trimmed Mean [64]	✗	⚠	⚠	✗	↓	Statistical Prior (Trimmed Mean Aggregation)
MultiKrum [7]	✗	⚠	⚠	✗	↓	Similarity-based (Euclidean Distance)
FLTrust [9]	✗	✓	⚠	✗	↓	Similarity-based (Cosine Similarity)
DPSGD [1]	⚠ ✓	✗	⚠ ✗	⚠ ✗	↑	Add perturbation to the local gradient
Gradient Pruning [69]	⚠ ✓	✗	⚠ ✗	⚠ ✗	↑	Zero-pad the local gradient
Tazza (Ours)	✓	✓	✓	✓	↓	Shuffle model parameters Cluster-aware aggregation

Table 1. Comparison of *Tazza* with existing federated learning frameworks and defense schemes.

## 2 BACKGROUND AND RELATED WORKS

### 2.1 Security Threats in Federated Learning

We begin by discussing background information on the two core security threats in federated learning: integrity and confidentiality attacks. We present a summary of existing federated learning frameworks and defense mechanisms that target to mitigate the aforementioned attacks in Table 1.

**Integrity Attacks.** Malicious clients can undermine the integrity of the federated learning process by compromising the reliability of model weights. Figure 1 (a) illustrates how such attacks operate. For instance, in data poisoning attacks, adversaries manipulate local models with altered data-label pairs (e.g., label flipping) to degrade global performance. In model poisoning attacks, they tamper with model weights by injecting noise (noise-injection) or scaling specific parameters (scaling attack) to distort outcomes [21]. Additionally, backdoor attacks involve training models to produce undesired outputs when triggered by specific input patterns [4]. Collectively, these adversarial activities are referred to as *integrity attacks* in this paper.

To mitigate integrity attacks, prior research has proposed secure model aggregation techniques leveraging statistical priors or similarity-based approaches (c.f., Table 1). Methods like Median [62] and Trimmed-Mean [65] aggregation exclude malicious updates by focusing on statistical measures rather than naive averaging, assuming that malicious updates are statistical outliers. Alternatively, similarity-based techniques such as Krum [7] use Euclidean distance to select updates with minimal deviation across models, while FLTrust [9] calculates trust scores based on cosine similarity with a verified, clean model stored at the server. Despite their strengths, these methods often discard valuable information in the updates, leading to suboptimal global model performance.

**Confidentiality Attacks.** Another significant security threat in federated learning systems is confidentiality attacks, which aim to infer and reveal local training data at the federated learning server. Figure 1 (b) illustrates the workflow of these attacks. Zhu et al. introduced DLG, demonstrating that training data can be reconstructed by analyzing the differences between the initial model distributed by the server and the updated model parameters returned by the local clients [70]. Specifically, DLG employs an optimization-based approach using L-BFGS to identify data that generates gradients minimizing the difference between the local model and the updated parameters, as shown in Figure 1 (b). Building on DLG, Geiping et al. proposed the Inverting Gradient attack, which incorporates the cosine similarity of the gradient and the total variation of the reconstructed image [25].

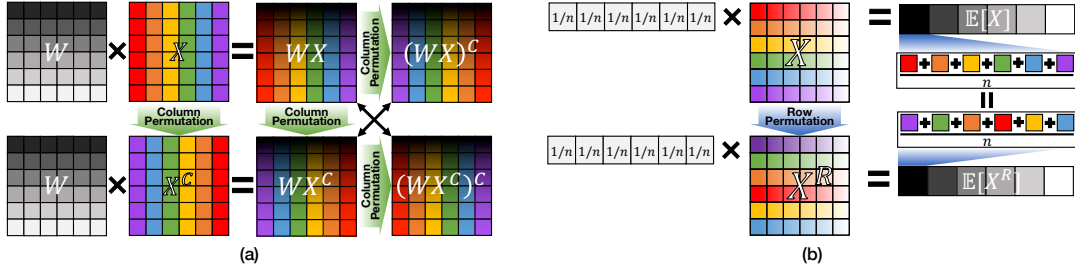


Fig. 2. (a) Visualization of the permutation equivariance property of matrix multiplication. The output’s column order follows the order of the input columns. (b) Visualization of the permutation invariance property of the average function. Results are not affected by the altered order of input rows. Best viewed in color.

To counter confidentiality attacks, widely adopted approaches include applying differential privacy [1], which adds controlled noise to model updates, and gradient pruning [70], which suppresses sensitive information in gradients during local training. However, these defense mechanisms often degrade model performance, as they manipulate original updates in ways that hinder convergence and accuracy [27]. Furthermore, such approaches often necessitate repetitive computations during local training, which not only delay the federated training process but also impose additional computational burdens on local devices (c.f., Table 1).

## 2.2 Permutation Equivariance/Invariance

We now explore the concepts of permutation equivariance and permutation invariance, which are fundamental to the approach presented in this work.

**Permutation Equivariance** refers to the property where the order of a function’s output aligns with the order of its input. Figure 2 (a) illustrates this concept using matrix multiplication, where  $C$  represents a column-reversed matrix. Specifically, the figure demonstrates that when the column order of the input matrix  $X$  is reversed ( $X \rightarrow X^C$ ), the resulting matrix multiplication outputs,  $WX$  (top) and  $WX^C$  (bottom), differ only in the column order, which corresponds to the input’s order.

Formally, if a function  $f(\cdot)$  satisfies permutation equivariance, for a given input  $X = \{x_1, x_2, \dots, x_N\}$  and a permutation function  $\pi(i) : \{1, 2, \dots, N\} \rightarrow \{1, 2, \dots, N\}$ , where  $\pi(i)$  is a bijective mapping, the lemma  $\pi(f(X)) = f(\pi(X))$  holds. Applying this to the case of matrix multiplication, the function  $f(X) = WX$  satisfies permutation equivariance with respect to the column order. Consequently,  $WX^C$  (i.e., shuffling order of input) is identical to  $(WX)^C$  (i.e., shuffling order of output).

**Permutation Invariance** describes a function that produces identical results regardless of the order of its input. For example, a function that computes the average of the elements in a given array is permutation invariant because the arrangement of elements does not influence the outcome. Figure 2 (b) illustrates this concept using the average operation in the context of matrix multiplication, where  $n$  represents the number of rows and  $R$  denotes a row-permuted version of the input. As shown, despite reordering the rows, the final result remains unchanged (i.e.,  $\mathbb{E}[X] = \mathbb{E}[X^R]$ ). Without loss of generality, if a function  $f(\cdot)$  satisfies permutation invariance, then for a given input  $X$  and a permutation function  $\pi(i)$ , the lemma  $f(X) = f(\pi(X))$  holds.

It is important to note that matrix multiplication, in general, is *not* a permutation invariant operation. Specifically, if the weights used in the multiplication are not uniform (e.g.,  $\frac{1}{n}$  for all elements, as in the averaging operation shown in Figure 2 (b)), the result will differ depending on the order of the rows. This is because

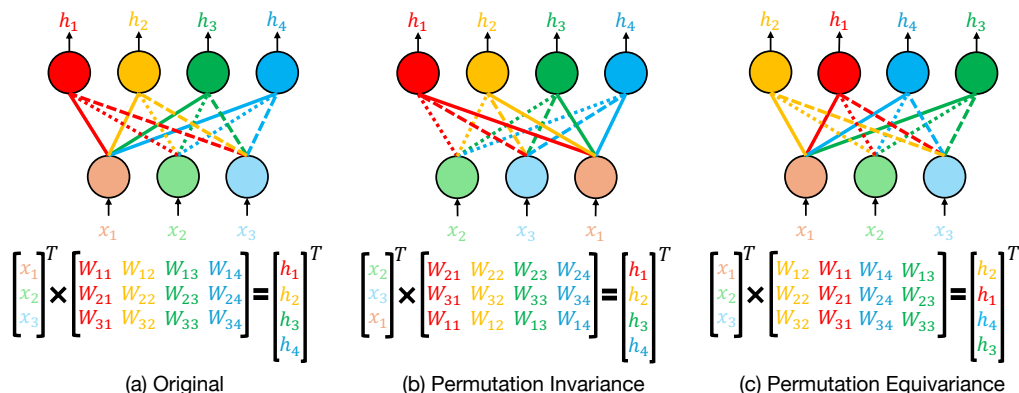


Fig. 3. Visualization of a simple neural network topology and its matrix computations to exemplify the permutation invariance and equivariance properties. (a) Original network architecture and computations. (b) Row-permuted operations, where the input nodes ( $x_1, x_2, x_3$ ) are rearranged to ( $x_2, x_3, x_1$ ), demonstrating the permutation invariance property as the network topology and output remain unchanged. (c) Column-permuted operations, where the output nodes are reordered, highlighting the permutation equivariance property, as the network maintains consistent output relationships regardless of the arrangement. Best viewed in color.

such weights can be interpreted as a weighted sum, being sensitive to the input arrangement, emphasizing the importance of exquisite shuffling operation in a neural network to retain the property.

**Neural Networks and Shuffling.** Modern neural networks exhibit an intriguing property that achieves nearly identical training results even when the arrangement of elements in the input data is shuffled, demonstrating similar behavior to permutation invariance [42, 59]. *Shuffling*, here, refers to rearranging the elements of a data sample, such as altering the position of pixels in an image. Similarly, reordering ground truth labels has minimal impact on training outcomes, reflecting characteristics similar to permutation equivariance. However, it is important to note that neural networks exhibit a *semi*-permutation equivariance and invariance property, as results are not perfectly identical but still closely adhere to these principles. This property arises primarily from the reliance of neural networks on matrix multiplication for most of their operations [29, 67].

In Figure 3, we visualize the topology and matrix computations of a simple neural network to provide deeper insights into its structural properties. Specifically, Figure 3 (a) depicts the original architecture and computations of the neural network, while Figures 3 (b) and (c) illustrate row-permuted and column-permuted operations, emphasizing the permutation invariance and equivariance properties, respectively.

By examining the nodes and edges in Figure 3 (a), we observe that these elements are interconnected in a fixed manner. Note that rearranging the input nodes, as illustrated in Figure 3 (b) (e.g.,  $\{x_1, x_2, x_3\} \rightarrow \{x_2, x_3, x_1\}$ ), does not alter the network topology since node connections remain intact. The structural integrity of the network is maintained given that the relationships between nodes and edges are preserved. Formulating the computation as  $X^T W$ , where  $X^T$  represents the transposed input vector ( $X_i$ ) and  $W$  denotes the weight matrix ( $W_{i,j}$ ), mathematically demonstrates that reordering the input vector  $x_i$  does not impact the model's output  $h_i$ . This property confirms the permutation invariance of a neural network.

On the other hand, when the output nodes are rearranged, as in Figure 3 (c), this operation corresponds to a column permutation in the weight matrix. Despite the reordering, the underlying network topology remains unchanged, and the outputs are consistent except for their order. This behavior exemplifies the permutation equivariance property of the neural network, where the outputs reflect the same relationships regardless of the node arrangement.

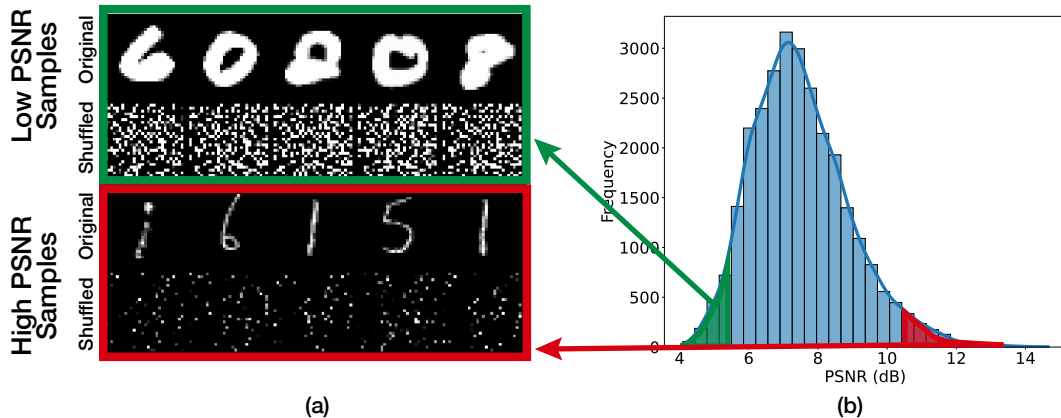


Fig. 4. (a) Bottom-5 (top green box) and Top-5 (bottom red box) PSNR samples from the MNIST dataset. (b) PSNR distribution between the original and shuffled images from the MNIST dataset (using 60K images).

Leveraging this property, neural networks can achieve similar training results with spatially shuffled data as with unshuffled data. Since shuffled data is semantically uninterpretable to humans, prior research has highlighted its potential to enhance system privacy. For instance, Amin et al. used permutation equivariance to secure medical image processing [3], while Xu et al. explored its applications in transformers for model encryption and privacy-aware split learning [64].

### 3 FEASIBILITY STUDY AND CORE IDEA

We now present our preliminary studies, which demonstrate the feasibility of permuting data during neural network training from the perspectives of *data privacy* and *model performance* preservation. Building on the insights gained from these experiments, we introduce the core concept underlying our proposed framework *Tazza*.

**Feasibility Study.** To evaluate the feasibility of leveraging shuffling methods for preserving data privacy, we measured the Peak Signal-to-Noise Ratio (PSNR) between original and shuffled samples in the MNIST dataset. For shuffling, we randomly rearranged the pixels in the input data following a consistent and fixed order applied uniformly across all samples. Figure 4 presents sample original/shuffled images and the distribution of measured PSNR values between 60,000 original and shuffled images. A high PSNR indicates structural similarity between two images, whereas a low PSNR suggests significant differences. As Figure 4 (a) shows, the shuffled samples do not retain the semantic information of the original images. Moreover, Figure 4 (b) shows that most samples exhibit low PSNR in the range of 6–8 dB. Even for the top-5 PSNR samples, the shuffled images remain semantically uninterpretable to human observers, confirming the effectiveness of shuffling in preserving data privacy.

Next, we trained a 3-layer MLP model for 20 epochs using two dataset configurations: one with original data and the other with shuffled data, as exemplified in Figure 4 (a). For the shuffling process, the test data and training data were shuffled using the same order across all samples. Figure 5 presents the average validation accuracy for 10 different random seeds. As the plots show, the model achieves (nearly) identical accuracy regardless of whether the input data were shuffled, demonstrating the neural network’s semi-permutation invariance property. This result suggests that data shuffling can preserve computation consistency in both training and inference, while effectively addressing user data privacy concerns since the training data is spatially shuffled which hinders the semantic information as shown in Figure 4.

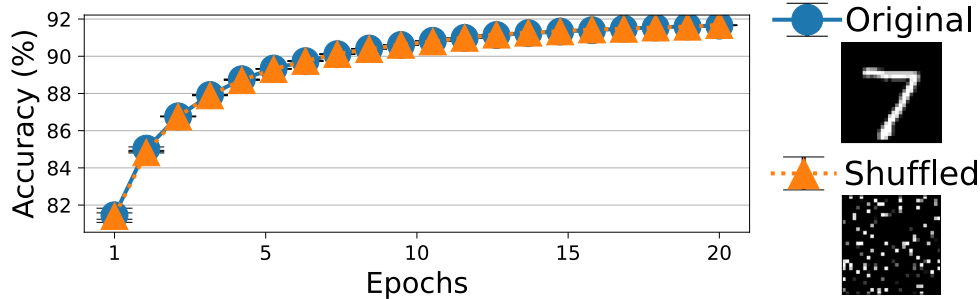


Fig. 5. Average accuracy of models trained with original data and shuffled data for 10 random seeds.

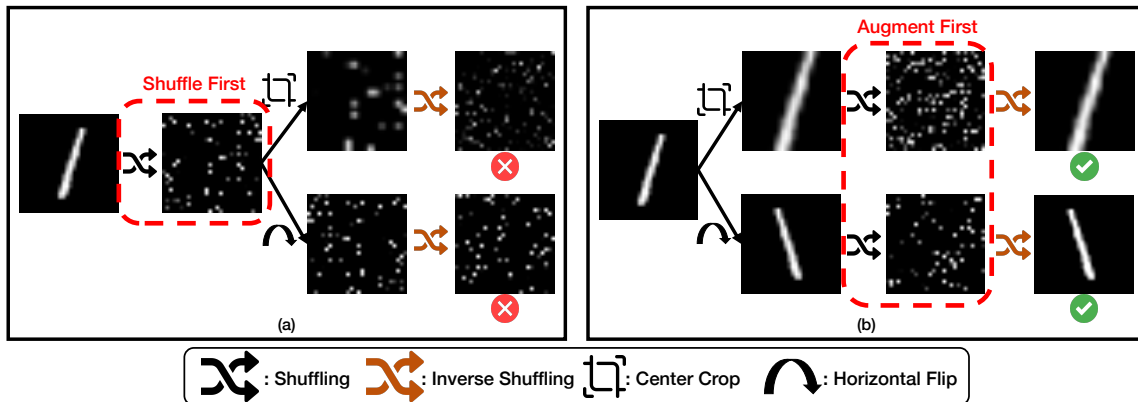


Fig. 6. Visualization of sample data illustrating the impact of operation order on the data semantics. (a) Shuffling applied *prior* to augmentation operations (center crop and horizontal flip), resulting in disrupted spatial coherence and semantically meaningless data. (b) Shuffling applied *after* the augmentation operations, preserving semantic integrity and highlighting the importance of processing order.

**Challenges and Core Idea.** As training results remain nearly identical even when using shuffled data, training models on shuffled inputs rather than original can be a plausible approach for preserving data confidentiality. However, while shuffling input data mitigates confidentiality attacks, it still introduces challenges related to computational overhead and system generalizability.

First, models trained on shuffled data require inputs to be shuffled during both training and inference, adding computational overhead for resource-constrained devices in federated learning systems. Second, standard data augmentation techniques, often essential for improving model performance and convergence, rely on spatial or locality-based assumptions (e.g., random cropping or horizontal flipping) [51, 57]. These techniques are incompatible with shuffled data, as shuffling disrupts spatial coherence. Consequently, precomputing shuffled data becomes impractical unless augmentation is specifically adapted to the applied permutation, increasing complexity and reducing generalizability.

To illustrate this, we present a visualization of samples subjected to shuffling and two commonly used augmentation techniques (i.e., center crop and horizontal flip) applied in different sequences. Figure 6 (a) and (b) depict scenarios where the shuffling operation is performed either prior to or after the augmentation steps, respectively. As demonstrated, applying shuffling prior to cropping or flipping disrupts the spatial coherence of the data, leading to semantically meaningless samples. Conversely, when shuffling is executed following the

augmentations, the semantic integrity of the data is preserved. This underscores the critical importance of the operational sequence in maintaining data utility.

To overcome these challenges, we exploit the interchangeability of shuffling data and shuffling *weights*, a property rooted in the permutation invariance of neural networks. Neural network weights trained on shuffled data inherently adapt to the shuffling rules of the input. By carefully rearranging these weights and leveraging the properties of permutation invariance and equivariance, the model can behave as if it were trained on unshuffled (original) data. Conversely, shuffling the weights of a model trained on unshuffled data enables it to operate equivalently with shuffled inputs, thereby preserving the confidentiality of the system.

This weight shuffling approach can alleviate the computational overhead by eliminating the need for repeated data shuffling operations during training and inference while maintaining compatibility with the original data. Additionally, this approach restores the applicability of standard data augmentation techniques, preserving the framework’s generalizability and reducing complexity.

## 4 THREAT MODEL

This work considers two key stakeholders in federated learning scenarios: clients and the server. Both clients and the server can potentially be victims or act as adversaries. Thus, we address two different types of attackers namely *integrity attacker*, and *confidentiality attacker*.

**Goals and Capability** First, an *integrity attacker* refers to a malicious client that aims to compromise the performance of the global model by injecting harmful information through tampered model updates. Integrity attackers can launch model or data poisoning attacks, manipulating the local training process by altering labels, training data, or model weights. Second, we consider an *honest-but-curious* server as a *confidentiality attacker*, which seeks to infer a client’s training data by exploiting the received information. Given that clients transmit their model updates to the server for aggregation, the attacker has access to the updates explicitly shared by the clients. Furthermore, there can be additional shared information, which can be any type of data that the clients are required to transmit for the global model training process (e.g., the amount of training data used).

**Assumptions** For the integrity attack, we assume that the attacker has no control over its device beyond the local training process. Specifically, the attacker cannot interfere with the weight aggregation, distribution, or client selection processes carried out by the federated learning server, nor can it access information from other benign clients, such as their data distribution, model weights, or updates. Finally, we assume that the proportion of attackers cannot exceed 50% of the total number of clients [21], all being common assumptions in prior work. In the case of a confidentiality attacker, the attacker cannot interfere with or access the local operations performed on clients, nor can it eavesdrop on network communications. Lastly, we note that both types of attackers make every effort to achieve their objectives and circumvent defense mechanisms, while the victim systems can operate cooperatively to prevent these attacks or leverage additional security features, for instance, peer-to-peer communication [61] and multi-party computation [69]. We note that the extensive lines of previous studies have tried to establish such features in practical, scalable, and efficient aspects; thus, we do not consider this as a strong assumption [28].

## 5 FRAMEWORK DESIGN

### 5.1 Overview of *Tazza*

We now detail the design of *Tazza*, a secure and efficient federated learning framework that simultaneously addresses integrity and confidentiality attacks. Specifically, *Tazza* features two core modules, *weight shuffling* and *shuffled model validation* and exploits the permutation equivariance and invariance properties of neural networks.

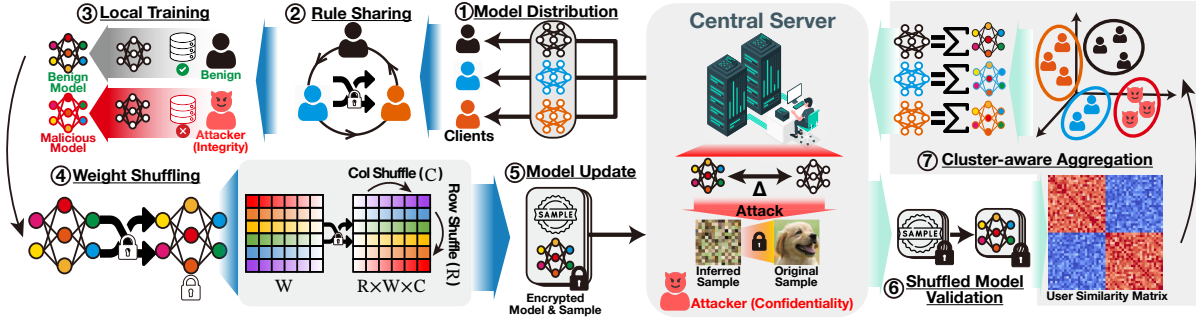


Fig. 7. Overall workflow of Tazza.

Figure 7 illustrates the overall workflow of *Tazza*: ① The federated learning server distributes a global model to each client. ② Clients selected to participate in training share a *shuffling rule* via a safeguarded peer-to-peer communication. As a communication-efficient approach, *Tazza* simply shares the random seed for generating the shuffling order (Sec 5.2). ③ Participants of the federated learning round train the neural network model with their locally collected data. ④ Upon completing local training, each participant shuffles its local model weights with respect to the shared rule to ensure the confidentiality of the training operations (*Weight Shuffling*-Sec. 5.3). ⑤ Participating clients transmit the shuffled model parameters and a small number of input samples (as small as one) to the server. We note that the input samples are also shuffled to prevent the confidentiality of the system from being compromised. ⑥ With the updated/shuffled models and data samples, the server performs an integrity check via *shuffled model validation* on the data samples using each client’s model by measuring the similarity of resulting output vectors (Sec. 5.4). Since models and data samples are shuffled to satisfy the permutation invariance of the neural network based on the shared shuffling rule in ②, the resulting output vectors are still legitimate. ⑦ Exploiting the similarity between the clients calculated in the previous step, *Tazza* employs a clustering algorithm to cluster the clients. As malicious and benign models exhibit different computation results, grouping the clients based on their similarity effectively assures that benign clients are not affected by malicious model updates.

To summarize, in Step ④, the weight shuffling process ensures that by shuffling the weights, the server is not able to infer information about the client’s local data through model analysis. Nevertheless, since weights are shuffled while preserving permutation invariance, the vectors calculated in Step ⑥ still remain valid. This enables the shuffled validation process to effectively identify malicious clients attempting poisoning attacks by clustering them in Step ⑦. In addition, despite the altered order, model aggregation can take place seamlessly as all clients are employing the same shuffling rule.

## 5.2 Shuffling Rule Sharing

Before delving into the detailed design of *Tazza*, we first address a potential issue regarding clients independently shuffling their model weights in differing orders, which would void the validation process and lead to degraded aggregated model performance. Therefore, it is important for clients to agree upon a unified weight-shuffling order. However, the challenge here is that if the server gains access to this unified shuffling rule, it could potentially revert the shuffled models to their original state, posing a security risk. To mitigate this, the core requirement for securing the system lies in establishing an information asymmetry between the server and clients regarding the shuffling rule. To achieve this, existing security mechanisms such as secure multi-party computation [69], zero-knowledge proofs [8], confidential computing [39], or peer-to-peer communication [11] can be employed

to fulfill this prerequisite. As previously mentioned, we assume that clients utilize these secure communication methods to exchange shuffling rules among themselves, ensuring that the server remains unaware of the specific shuffling details.

Specifically, *Tazza* employs a Practical Byzantine Fault Tolerant (PBFT) mechanism [11] for exchanging its shuffling rules. The server selects one participating client as the head, which distributes a shuffling rule to others. Participants who receive the rule then broadcast the rule to non-participating clients to reach a consensus. Even if a malicious client is chosen as the leader, PBFT ensures that consensus is achieved and the shuffling rule remains secure and consistent across all clients, despite potential attacks.

In detail, during each federated training round, clients exchange two shuffling rules to support model updates. First, the model distributed by the server is encrypted using the shuffling rule from the previous round, which clients retrieve through secure communication from clients that have participated in the specific round. Additionally, clients share a new shuffling rule among the current round’s participants to encrypt the locally updated model. As previously noted, the shared rules are lightweight, being as simple as a single random seed to minimize the communication overhead.

### 5.3 Weight Shuffling

The weight shuffling module in *Tazza* aims to prevent data leakage while preserving computational correctness by leveraging permutation equivariance and invariance. As the name suggests, this operation shuffles the neural network weights of a model updated at the client before sharing them with the server for aggregation. For clarity, we explain the weight shuffling process in the context of matrix multiplication, given its predominant role in neural network computations. It is worth noting that implementation details of this module can vary depending on the baseline federated learning model architecture due to differences in design and computational complexity, as discussed in Section 6.

In essence, weight shuffling in *Tazza* consists of two core operations: row shuffling and column shuffling. Consider a matrix multiplication between the input matrix  $\mathbf{X} \in \mathbb{R}^{N \times d}$  and the weight matrix  $\mathbf{W} \in \mathbb{R}^{d \times h}$ , where  $N$ ,  $d$ , and  $h$  denote the number of vectors, input dimension, and embedding dimension, respectively. To shuffle the weight rows, a row-permutation matrix  $\mathbf{R}$  can be applied to  $\mathbf{W}$  (i.e.,  $\mathbf{R} \times \mathbf{W}$ ). This operation is computationally equivalent to directly shuffling the input, thereby ensuring data confidentiality. Here, we note that a permutation matrix  $\mathbf{R}$  satisfies the following lemma:  $\mathbf{R}^T \mathbf{R} = \mathbf{I}$  where  $\mathbf{I}$  denotes the identity matrix. Based on this, by applying the same permutation to  $\mathbf{X}$  via  $\mathbf{R}^T$  (i.e.,  $\mathbf{X} \times \mathbf{R}^T$ ), the computation results remain unchanged due to the property of permutation invariance, since  $(\mathbf{X} \mathbf{R}^T)(\mathbf{R} \mathbf{W}) = \mathbf{X} \mathbf{I} \mathbf{W} = \mathbf{X} \mathbf{W}$  (c.f., Figure 3 (b)).

The weights can be shuffled further with respect to the columns by multiplying the weight matrix  $\mathbf{W}$  with a column-permutation matrix  $\mathbf{C}$  (i.e.,  $\mathbf{W} \times \mathbf{C}$ ). Since column shuffling affects only the column order of the output and not the computation itself, no additional permutation needs to be applied to the input (c.f., Figure 3 (c)). However, when considering the bias term  $\mathbf{b} \in \mathbb{R}^h$  in a linear layer (i.e.,  $\mathbf{X} \times \mathbf{W} + \mathbf{b}$ ), the same column permutation must be applied to  $\mathbf{b}$  to ensure proper alignment with the shuffled weights. Since the output of a layer serves as the input for the subsequent layer, the column shuffling order of the current layer can be directly inherited as the row shuffling order for the weights of the next layer.

This shuffling operation for matrix multiplication (i.e., linear layers) leverages permutation invariance and equivariance, which form the foundation of most neural network computations. However, simply uniformly applying this approach to all weights may not always work as intended. This is because, while the underlying principle remains consistent, specific behaviors and designs of models can vary. We elaborate on how this shuffling operation can be adapted for various complex and advanced neural network architectures in Section 6.

---

**Algorithm 1:** Cluster-Aware Aggregation in *Tazza*

---

**Input:** Client models and pseudo-cluster labels for round  $t$ , global cluster labels  $G$

**Output:** Updated global cluster labels and aggregated models per cluster

```
1 Initialize: New global cluster set  $G_{\text{new}} \leftarrow G$ ;  
2 foreach pseudo-cluster  $C_p$  in round  $t$  do  
3   Classify clients in  $C_p$ :  
4    $C_{\text{new}} \leftarrow$  clients without global labels;  
5    $C_{\text{existing}} \leftarrow$  clients with global labels;  
6   if  $C_{\text{existing}} = \emptyset$  then  
7     Assign a new global cluster  $g_{\text{new}}$  to all clients in  $C_p$ ;  
8     Update  $G_{\text{new}} \leftarrow G_{\text{new}} \cup \{g_{\text{new}}\}$ ;  
9   else  
10    Identify the dominant global label  $g_{\text{dom}}$  in  $C_{\text{existing}}$ ;  
11    Assign  $g_{\text{dom}}$  to all clients in  $C_p$ ;  
12    if clients with different global labels are grouped in  $C_p$  then  
13      Reassign overlapping clients in  $C_p$  to a new merged cluster;  
14      Update  $G_{\text{new}}$  with the merged cluster;  
15 foreach global cluster  $g$  in  $G_{\text{new}}$  do  
16   Perform model aggregation for clients in  $g$ ;  
17 return Updated global clusters  $G_{\text{new}}$  and aggregated models;
```

---

## 5.4 Integrity Check

Integrity check in *Tazza* is designed to identify and isolate malicious models from benign ones through two key steps: *shuffled model validation* and *cluster-aware aggregation*.

**5.4.1 Shuffled Model Validation.** In the Shuffled Model Validation process, the server utilizes client-provided samples as inputs to the uploaded models. As previously mentioned, these data samples are also shuffled to obscure their semantics, ensuring data confidentiality. Despite this obfuscation, the corresponding weight shuffling maintains computational validity, allowing the server to trust the outputs based on the assumed correctness of the shuffle rules. If an attacker uploads models with mismatched data and weight shuffle orders, inconsistent results will emerge, distinguishing these models from legitimate ones. This forces attackers to comply with the correct shuffle rules to avoid exclusion during subsequent stages.

Malicious models produce outputs that deviate from those of benign models, revealing distinctive patterns. *Tazza* identifies such deviations by computing pairwise cosine similarity among the output vectors of all models [48]. Malicious models typically exhibit lower cosine similarity with benign ones, providing a basis for their classification and isolation. Clients are then clustered based on their pairwise cosine similarities, with the similarity matrix ( $S$ ) transformed into a distance matrix ( $1 - S$ ) to interpret similarity as a distance metric, which is used as input to the DBSCAN algorithm [20]. *Tazza* leverages DBSCAN for its ability to identify outliers and its independence from predefined cluster numbers, making it particularly well-suited for federated learning scenarios where the presence of attackers is unknown.

**5.4.2 Cluster-aware Aggregation.** Finally, we implement cluster-aware aggregation to fully segregate malicious models from benign ones. Algorithm 1 presents the pseudo-code for the cluster-aware aggregation process.

In each federated learning round, computed cluster labels from DBSCAN serve as *pseudo-labels*, reflecting the similarities among clients within that round only. These labels are independent across rounds (e.g., labels from round  $t$  have no relation to those from round  $t + 1$ ). To ensure consistency, *Tazza* assigns global cluster labels by leveraging clustering histories, enabling effective cross-round clustering. Clients are categorized into two groups: (1) those participating for the first time, who lack a global cluster label, and (2) those with prior participation and an assigned global cluster (line 3-5 in Algorithm 1).

Upon performing shuffled model validation, if all clients in a cluster are first-time participants without any global cluster assignment, *Tazza* creates and assigns new global clusters (line 6-8 in Algorithm 1). Conversely, if a pseudo-cluster contains clients with pre-existing global cluster labels, all clients in the cluster are assigned to the global cluster label of those clients (line 10-11 in Algorithm 1).

Furthermore, if clients who were previously part of different global clusters are grouped in the same pseudo-cluster during the current round, *Tazza* merges their global clusters. However, instead of merging all clients from both clusters indiscriminately, *Tazza* adopts a conservative approach by reassigning only the overlapping clients to the new cluster (line 12-14 in Algorithm 1). This precautionary strategy ensures that a single attacker infiltrating a benign cluster cannot lead to all attackers being included in the same benign cluster.

When global clusters are assigned for participating clients, *Tazza* performs aggregation within each cluster based on the clustering results, producing an updated model for each cluster (line 15-16 in Algorithm 1). We note that *Tazza* employs averaging as the aggregation algorithm while alternative methods such as median or trimmed mean can also be applied, offering flexibility in system design. By aggregating models only within the same cluster, *Tazza* prevents compromised models from contaminating the global model shared across other clusters. We also point out that, although the server is unaware of how model parameters are shuffled, it can still seamlessly aggregate these parameters since they are organized according to consistent rules as discussed in Section 5.3.

This cluster-specific aggregation ensures that the integrity of the federated learning system is maintained, as malicious models cannot propagate their impact to benign clusters [37]. Furthermore, by leveraging shuffled model validation, *Tazza* achieves this robust defense without exposing or interpreting the semantics of clients' data, thereby preserving both system security and data confidentiality. Overall, this dual protection reinforces *Tazza's* effectiveness in safeguarding federated learning processes against security threats.

## 6 IMPLEMENTATION

As previously noted, details of the weight shuffling operation (and implementations) can vary for different model architectures. In this section, we provide a detailed explanation of the weight shuffling process for representative architectures.

**Multi-layer Perceptron (MLP).** As a simple architecture, we demonstrate the weight shuffling operation in an MLP. In an MLP with  $L$  layers, the output  $y$  is computed as follows:

$$\begin{aligned} h^{(0)} &= x, \\ h^{(l)} &= \sigma(h^{(l-1)}W^{(l)\top} + b^{(l)}), \quad l = 1, \dots, L - 1, \\ y &= h^{(L-1)}W^{(L)\top} + b^{(L)}, \end{aligned} \tag{1}$$

Here,  $h^{(l)}$  denotes the activations of the  $l$ -th layer,  $W^{(l)}$  represents the weight matrix associated with the  $l$ -th layer,  $b^{(l)}$  is the bias vector for the  $l$ -th layer, and  $\sigma(\cdot)$  is a non-linear activation function such as ReLU, sigmoid, or tanh.

A critical observation is that commonly used activation functions are parameter-free and permutation-equivariant, meaning their intrinsic behavior remains unaffected by input shuffling. As a result, activation

```

def shuffle_linear(fc:nn.Module, shuffle_rule:int):
    '''
    Pseudo-code for linear layer (MLP) weight shuffling
    fc = (input_dim, hidden_dim) shaped linear layer
    (i.e., nn.Linear(input_dim, hidden_dim))
    '''
    # fix random seed to generate unified shuffling indices across clients
    torch.manual_seed(shuffle_rule)
    hidden_dim, in_dim = fc.weight.size()
    in_shuffle_idx = torch.randperm(in_dim)
    # unshuffle_idx = torch.argsort(in_shuffle_idx) # to unshuffle
    hidden_shuffle_idx = torch.randperm(hidden_dim)
    fc.weight = torch.nn.Parameter(fc.weight[hidden_shuffle_idx][:, in_shuffle_idx])
    fc.bias = torch.nn.Parameter(fc.bias[hidden_shuffle_idx])
    return fc

```

Listing 1. PyTorch implementation of the weight shuffling module for a linear layer.

functions can be excluded from considerations in weight shuffling operations. This leaves the linear transformations in each layer, represented as matrix multiplications ( $h^{(l-1)}W^{(l)\top}$ ), as the primary focus. The weight matrices and bias vectors in these transformations can be shuffled according to the previously outlined strategies, ensuring that computational outcomes remain consistent despite weight shuffling. By applying this shuffling mechanism iteratively across layers, the entire MLP architecture retains compatibility with weight shuffling operations, preserving computational integrity while safeguarding model confidentiality.

Listing 1 presents the PyTorch [50] implementation of weight shuffling for the affine linear transformation layer, defined as  $f(\mathbf{x}) = \mathbf{x}\mathbf{W}^\top + \mathbf{b}$ . To minimize both memory and computational overhead, particularly given the resource-constrained nature of mobile and embedded devices deployed in ubiquitous applications, we replace explicit permutation matrix multiplication with index permutation. Notably, since the linear transformation layer relies on fundamental operations, such as matrix multiplication and addition, that are widely used in neural network architectures, this approach can be easily extended to more complex and advanced architectures without loss of generality.

**Sequential Models (RNN and LSTM).** For recurrent sequential models such as RNNs and LSTMs, the weight shuffling process is similar to that of MLPs, with one key distinction: the inclusion of hidden state operations. These operations enable sequential models to capture and process temporal dependencies in input data. Figure 8 illustrates the fundamental operation of a recurrent model (e.g., RNN), where the next output is computed by integrating the current input ( $x_t, W_{ih}$ ) with the hidden state vector from the previous time step ( $h_{t-1}, W_{hh}$ ). Despite this added complexity, the core computations in sequential models are rooted in matrix multiplications. This ensures that they, like MLPs, exhibit permutation equivariance and invariance properties, allowing weight shuffling to be applied without compromising computational correctness.

Notably, this property extends beyond RNNs to other popular sequential architectures, such as LSTMs, Bi-LSTMs, and GRUs. These models rely on matrix operations for processing both inputs and hidden states, making them equally compatible with weight shuffling techniques.

**Transformers.** Transformers, a widely used modern neural network architecture, operate in three main steps, as depicted in Figure 9. First, the input is segmented into a sequence of tokens, which are passed through a linear embedding layer to generate token embeddings. These embeddings are then processed by multiple encoder layers

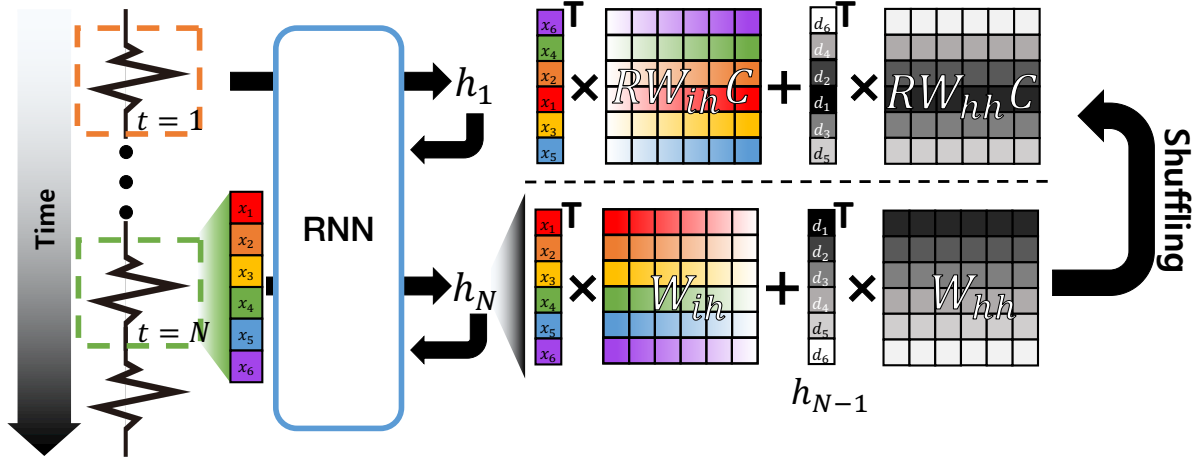


Fig. 8. Workflow of weight shuffling on a sequential model. For simplicity, we omit the bias addition.

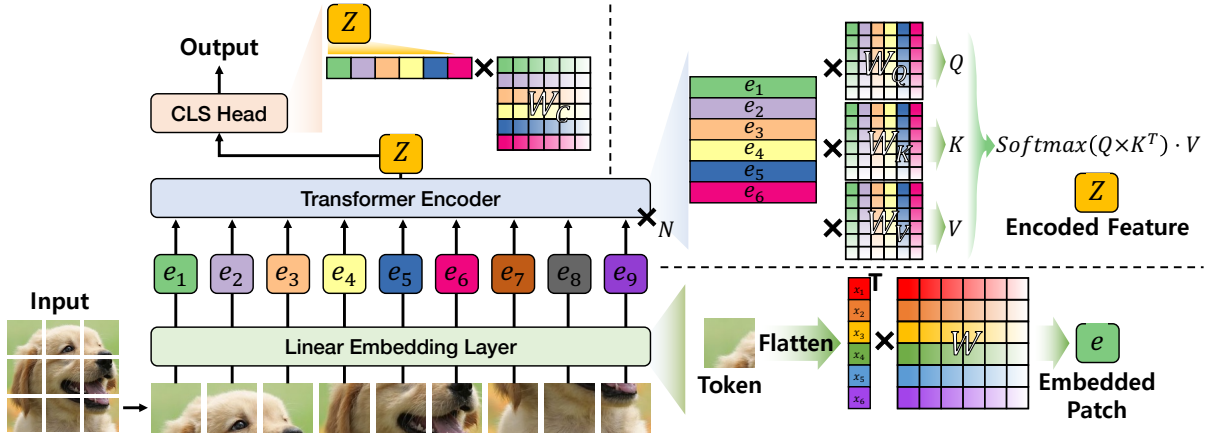


Fig. 9. Workflow with a transformer baseline. For clarity, we omit the bias addition and normalization.

that analyze the input. Each encoder employs a multi-head attention mechanism comprising three learnable matrices:  $W_Q$  (query),  $W_K$  (key), and  $W_V$  (value). Finally, the encoded feature representation,  $Z$ , is fed into the classification head (i.e., CLS Head) to produce the final output. Importantly, the encoded feature  $Z$  preserves the order of the input tokens, ensuring the model’s output aligns with the input sequence.

From a data perspective, shuffling can be applied at two levels: *intra-token* and *inter-token*. At the intra-token level, individual elements within a token are permuted. At the inter-token level, the sequence order of tokens is rearranged. Importantly, since all tokens pass through a linear embedding layer—essentially a matrix multiplication operation—the permutation invariance property of matrix multiplication ensures that identical computational results can be achieved by shuffling the embedding weights accordingly.

For inter-token shuffling, the sequential order of tokens is initially preserved during the attention mechanism (e.g., row order  $e_1, e_2, \dots, e_n$ ), where spatial or sequential positions are learned and encoded. However, in the final CLS Head, these positional features determine the model’s predictions. Consequently, inter-token shuffling can

be achieved by appropriately shuffling the weights of the classification head, ensuring consistent results while altering the token order.

We note that operations beyond the matrix multiplications discussed above (e.g., layer normalization, softmax) exhibit permutation equivariance (e.g., the softmax function) or permutation invariance (e.g., mean and variance computations in layer normalization). Consequently, these operations are unaffected by weight shuffling, ensuring that the computational results remain consistent. This allows *Tazza* to uphold not only the confidentiality of client data but also the integrity of the system.

## 7 EVALUATION

Now we evaluate *Tazza* with thorough and extensive experiments with four datasets and various comparison baselines.

### 7.1 Experiment Setup

**Dataset and Model.** We evaluate *Tazza* using four datasets with corresponding model architectures suitable for mobile federated learning scenarios as we detail below.

- **MNIST [15]** dataset consists of 60,000 training and 10,000 test grayscale handwritten digit images with  $28 \times 28$  pixel resolution. We use a 3-layered MLP [53] for evaluating MNIST.
- **CIFAR10 [31]** is a benchmark dataset consisting of 60,000  $32 \times 32$  pixel color images, categorized into 10 distinct classes. For this dataset, we use the MLP-Mixer [59] as the model, a design similar to the Vision Transformer but substituting self-attention blocks with MLP-based layers.
- **STL10 [14]** consists of 13,000 natural images across 10 classes, with a resolution of  $96 \times 96$  pixels. Its higher resolution makes it ideal for assessing *Tazza*'s scalability with image resolution. For this dataset, we employ Vision Transformer [16] to manage the increased complexity.
- **MIT-BIH Arrhythmia Database [40, 41]** is a widely used electrocardiogram (ECG) benchmark dataset comprising approximately 70K five-second ECG signals. We implement an RNN [54] to classify three arrhythmia types along with normal cardiac patterns. This dataset is utilized to explore the potential extension of *Tazza* to mobile/embedded applications that deal with time-series inputs [35, 49].

**Baselines.** For confidentiality attacks, we evaluate three baseline defense mechanisms: no defense, gradient pruning [70], and differential privacy [1, 17]. Gradient pruning zeros out small-amplitude gradients to reduce data leakage but requires a carefully balanced pruning ratio; higher ratios mitigate leakage but risk discarding useful knowledge, impacting both performance and convergence. Differential privacy, implemented via DPSGD [1], adds perturbation to gradients to obscure sensitive information, with perturbation levels divided into small, medium, and large, as in prior work [1]. Similar to gradient pruning, differential privacy also requires careful tuning of perturbation levels to balance between accuracy and privacy.

For integrity attacks, we use FedAvg [38] as a baseline, representing a naive model aggregation scenario. Specifically, FedAvg does not employ security mechanisms, leaving it vulnerable to malicious updates. We also evaluate robust aggregation methods leveraging statistical priors, including Median and Trimmed Mean [65]. Median replaces averaging with the median to mitigate extreme outlier influence, while Trimmed Mean excludes outliers before averaging, reducing the impact of malicious updates. Additionally, we compare *Tazza* with MultiKrum [7] and FLTrust [9], which are representative frameworks for similarity based approaches. MultiKrum selects updates with the smallest pairwise Euclidean distances after discarding the most distant ones. FLTrust assigns trust scores based on cosine similarity with a server-trained reference model, adjusting aggregation weights to suppress malicious updates.

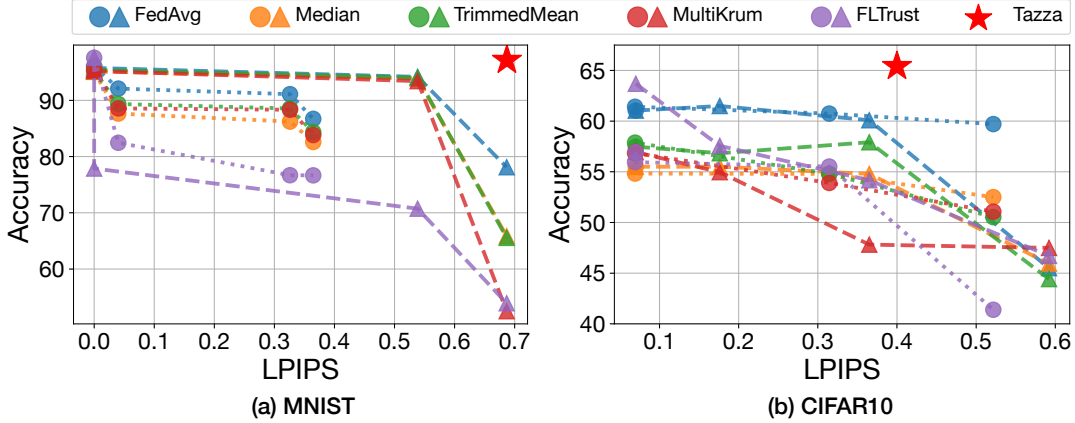


Fig. 10. LPIPS and accuracy of varying federated learning configurations.  $\blacktriangle$  and  $\bullet$  denote applying gradient pruning and DPSGD, respectively.

**Attack Methods.** For confidentiality attacks, we use the inverting gradient attack [25] for 100 test samples as a baseline. This method reconstructs training data by optimizing inputs to produce gradients similar to those sent by the client, achieving state-of-the-art performance with minimal additional assumptions [27].

For integrity attacks, we evaluate three poisoning attack types: label flipping, noise injection, and backdoor attacks [21]. In label flipping, the labels of a subset of training data are altered to mislead the locally trained model. Noise injection introduces random noise into the model parameters before they are sent to the server, aiming to degrade the global model’s performance. Backdoor attacks embed specific triggers into the training data, causing the model to behave maliciously when exposed to those triggers.

**Miscellaneous Configurations.** Throughout the evaluation, unless otherwise specified, datasets are distributed across 100 clients, consisting of 25 attackers, with data shared via a Dirichlet distribution with  $\alpha=0.5$  [26]. In each federated learning round, 10 participants are selected, and their models are trained locally for 5 epochs using the Adam optimizer [30] with a learning rate of  $1e-3$  and a batch size of 64. Besides the evaluations performed on real embedded computing platforms in Section 7.5, all experiments were conducted on a server with an NVIDIA RTX 2080 GPU, an Intel Xeon Silver 4210 CPU 2.20GHz, and 64GB RAM.

## 7.2 Overall Performance

To evaluate the overall performance of *Tazza*, we conducted experiments using the MNIST-MLP and CIFAR10-Mixer configurations with 75 benign clients and 25 label-flipping attackers (i.e., integrity attack), totaling 100 clients. To understand *Tazza*’s confidentiality-preserving capabilities, the server executed an inverting gradient attack. The effectiveness of the attack was measured using Learned Perceptual Image Patch Similarity (LPIPS) [68], which quantifies semantic distance in image data. Lower LPIPS values indicate greater similarity between the original training samples and those reconstructed by the attack, signifying higher attack success.

Figure 10 presents the global model accuracy under label-flipping attacks and the LPIPS across various integrity and confidentiality defense schemes. Additionally, since each cluster in *Tazza* has distinct model parameters, we report the average accuracy of the global model on the global test dataset across clusters that contain at least one benign client. The legend indicates different integrity defense schemes, with triangle ( $\blacktriangle$ ) and circle ( $\bullet$ ) markers representing confidentiality defense schemes using gradient pruning and DPSGD, respectively. Gradient pruning is applied with pruning ratios of 70%, 90%, and 99%, while DPSGD uses three perturbation levels: small, medium, and large, as outlined in prior work [1]. Each scheme includes three plots: the leftmost plot corresponds

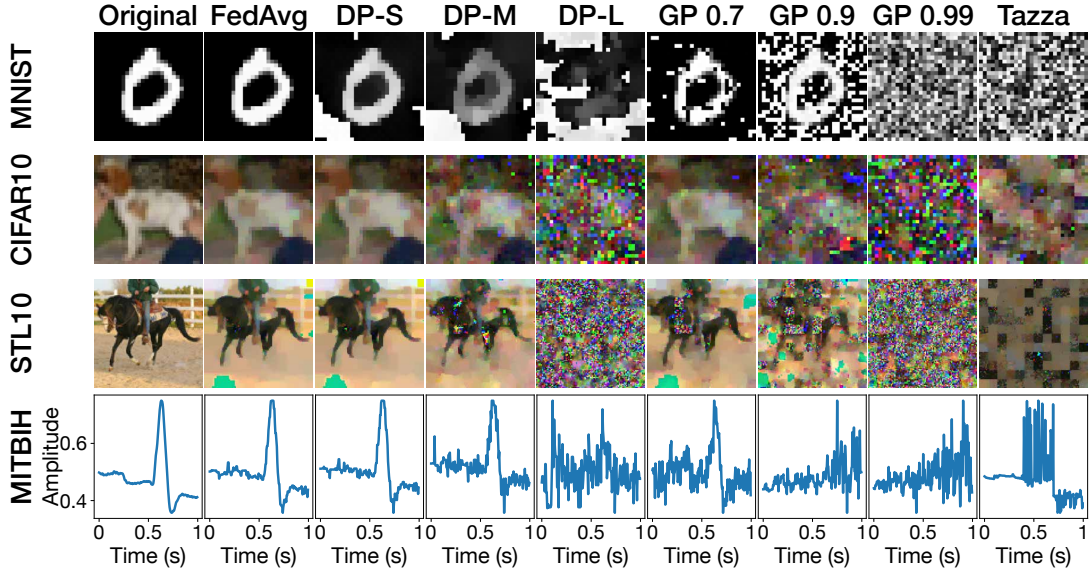


Fig. 11. Sample confidentiality attack results for different dataset/defense configurations.

		FedAvg	GP 0.9	DP-M	<b>Tazza</b>
Avg PSNR (↓)	MNIST	47.08±12.33	<b>4.92±0.53</b>	6.88±2.17	4.95±0.21
	CIFAR10	18.11±6.77	13.17±3.73	15.60±4.01	<b>11.74±2.92</b>
	STL10	12.21±4.88	10.23±2.33	12.14±4.67	<b>9.91±2.38</b>
	MITBIH	23.56±11.09	<b>-7.37±3.78</b>	19.33±13.39	17.01±8.74
Best PSNR (↓)	MNIST	61.28	6.34	14.77	<b>5.31</b>
	CIFAR10	30.46	<b>20.47</b>	24.33	21.12
	STL10	21.32	<b>15.15</b>	20.08	16.18
	MITBIH	35.35	<b>0.08</b>	32.34	22.69
Avg LPIPS (↑)	MNIST	0.04±0.16	0.69±0.04	0.52±0.09	<b>0.75±0.02</b>
	CIFAR10	0.36±0.24	0.61±0.10	0.51±0.12	<b>0.62±0.07</b>
	STL10	0.63±0.17	0.73±0.07	0.68±0.12	<b>0.75±0.05</b>
Best LPIPS (↑)	MNIST	0.00	0.54	0.33	<b>0.69</b>
	CIFAR10	0.07	0.37	0.31	<b>0.40</b>
	STL10	0.34	<b>0.62</b>	0.50	0.58

Table 2. Average and best PSNR/LPIPS between original and inferred sample results from confidentiality attack for different dataset/defense configurations.

to the weakest confidentiality defense configuration (70% pruning for gradient pruning and small perturbation for DPSGD), while the rightmost plot represents the strongest configuration (99% pruning for gradient pruning and large perturbation for DPSGD).

Existing confidentiality defense mechanisms improve data privacy, achieving higher LPIPS values, but often result in reduced accuracy. In contrast, *Tazza* achieves both high LPIPS and high accuracy, demonstrating its robustness against integrity and confidentiality attacks.

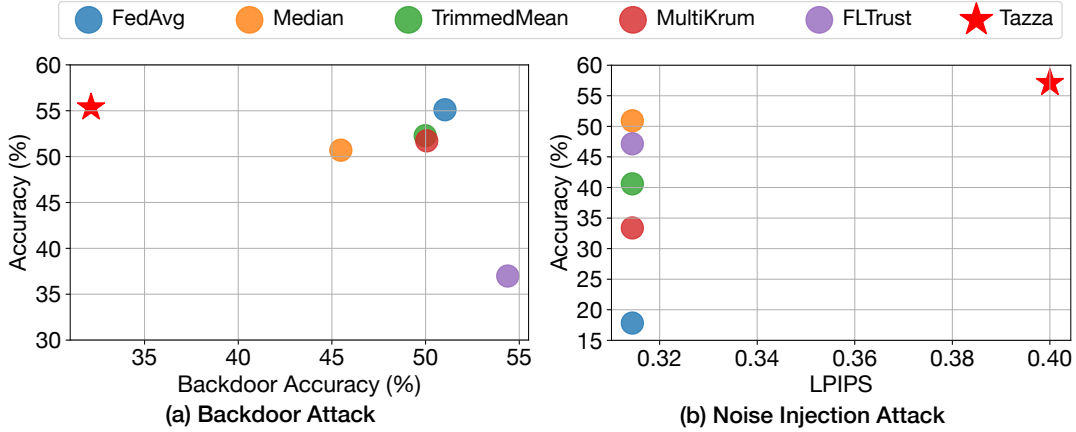


Fig. 12. (a) Backdoor accuracy and global model accuracy for different defense schemes against backdoor attack. (b) LPIPS and accuracy of different defense mechanisms under noise injection attack.

### 7.3 Confidentiality Attack Mitigation

To evaluate the efficacy of *Tazza* in mitigating confidentiality attacks, we measured PSNR and LPIPS between the original training samples and those inferred from the attack. PSNR assesses structural similarity, while LPIPS evaluates semantic distance for image data. Note that, as LPIPS is specific to images, only PSNR is reported for the MIT-BIH time-series dataset. Table 2 presents the average and best PSNR and LPIPS for various dataset and defense scheme configurations. The best values represent the most similar samples among the 100 used in the experiments. Higher PSNR and lower LPIPS indicate greater similarity between inferred and original samples.

As shown in Table 2, FedAvg without defense mechanisms results in high PSNR and low LPIPS, indicating substantial local data leakage. In contrast, defenses such as gradient pruning with 90% pruning (GP 0.9), DPSGD with medium perturbation (DP-M), and *Tazza* demonstrate competitive reductions in PSNR and increases in LPIPS, effectively mitigating confidentiality attacks. Notably, while gradient pruning and differential privacy face challenges in balancing model accuracy with confidentiality, *Tazza* successfully defends against attacks without compromising accuracy.

Figure 11 presents the inferred training samples generated by a gradient inversion attack at the server. In the absence of a defense mechanism (FedAvg), the local training data are completely exposed, significantly compromising the confidentiality of federated learning systems. Methods such as DPSGD with large perturbation (DP-L), pruning 99% of the local gradient effectively mitigate the gradient inversion attack, preserving the privacy of the training data while sacrificing the model training performance as noted earlier. On the other hand, when employing relatively weak defense mechanisms such as gradient pruning with pruning ratios 70% and 90% (GP 0.7, 0.9) or DPSGD with smaller perturbations (DP-S, M), the inferred samples still reveal interpretable semantic information, though with reduced visual clarity, requesting the need for stronger privacy-preserving techniques. As *Tazza*'s samples in Figure 11 show, our proposed approach effectively conceals semantic information embedded for both STL10-ViT and MIT-BIH-RNN configurations, suggesting its potential usage in high-resolution image and time-series data-based applications.

### 7.4 Integrity Attack Mitigation

In this section, we evaluate *Tazza*'s robustness against various integrity attacks, specifically focusing on noise addition and backdoor attack scenarios. The experiments exploit the CIFAR10-Mixer configuration with medium-level DPSGD as the confidentiality defense mechanism for all baselines. For the backdoor attack, attackers assign

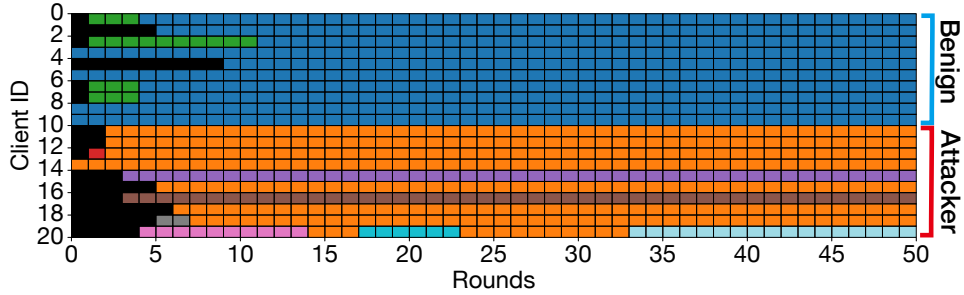


Fig. 13. Visualization of client clustering. Different colors denote different clusters. Best viewed in color.

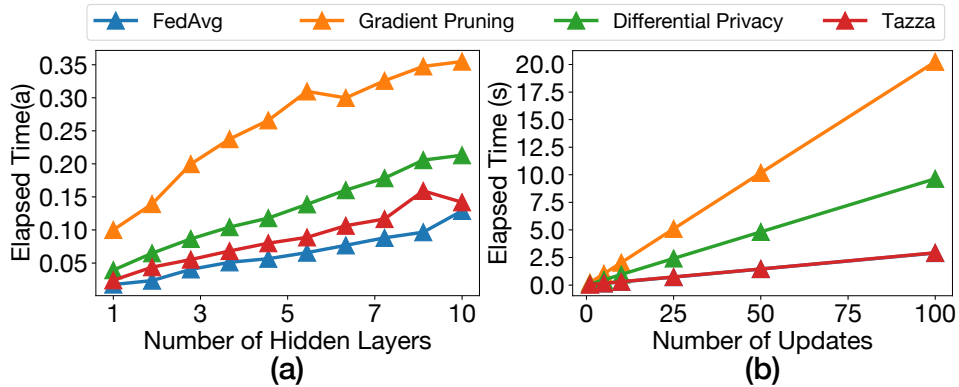


Fig. 14. Latency of different confidentiality attack mitigation schemes with varying (a) hidden layer counts and (b) the number of local training updates.

specific labels to samples by injecting a  $4 \times 4$  red square patch into the upper-left corner of 50% of their training data as the backdoor trigger [32]. For the noise addition attack, Gaussian noise with a scaling factor of 0.25 is injected into the model weights before they are uploaded to the server.

Figure 12 presents the global model accuracy (higher values indicate better performance on normal samples; y-axis) and backdoor accuracy (lower values indicate better attack mitigation for triggered samples; x-axis). As shown, baseline methods struggle to effectively counter backdoor attacks and often sacrifice global accuracy. On the other hand, *Tazza* achieves an 18.89% reduction in backdoor accuracy compared to the FedAvg baseline while maintaining a global model accuracy of 55.37%.

To effectively show how benign and malicious clusters are separated in *Tazza*, we devise another experiment with 10 benign clients (Clients 1-10) and 10 backdoor attackers (Clients 11-20) training the MNIST-MLP configurations for 50 federated learning rounds. We visualize the cluster allocation for each client at each training round in Figure 13. The illustration clearly shows that *Tazza* effectively isolates benign clients from malicious attackers demonstrating the efficacy of *Tazza* in mitigating integrity attacks.

### 7.5 Scalability on Real Embedded Platforms

To evaluate the scalability of *Tazza* and suitability for real-world applications, we conducted experiments on three embedded computing platforms: Raspberry Pi 3B [52], Nvidia Jetson Nano [43], and Nvidia Jetson TX2 [44]. These experiments focus on the computational latency of executing *Tazza* compared to widely used attack mitigation schemes.

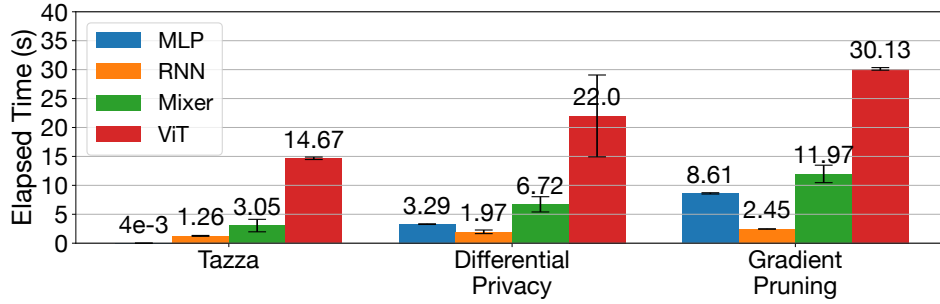


Fig. 15. Latency of different confidentiality attack mitigation schemes with varying model architectures.

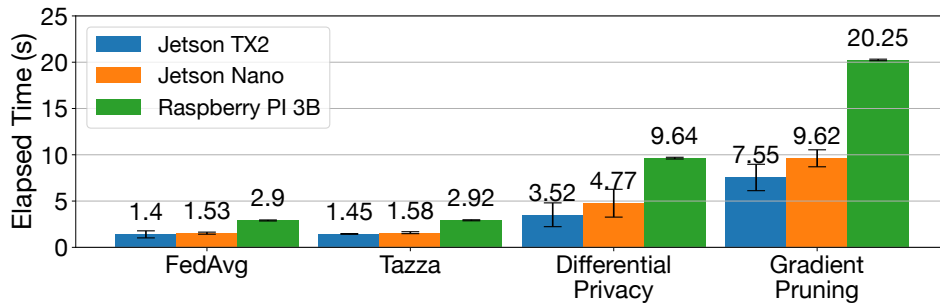


Fig. 16. Latency of varying confidentiality attack mitigation schemes for different embedded platforms.

Figure 14 plots the computational latency of various defense mechanisms across different network depths (Figure 14 (a)) and numbers of mini-batch updates during local training (Figure 14 (b)) using the MNIST-MLP configuration on the Raspberry Pi platform. In Figure 14 (a), latency increases with neural network depth, exhibiting a near-linear trend across all methods. However, *Tazza* demonstrates a less-steep increase compared to alternative defense schemes such as gradient pruning and differential privacy. Similarly, Figure 14 (b) shows a similar trend with the number of mini-batch updates, where *Tazza*'s advantage becomes even more pronounced. This efficiency comes from the fact that approaches such as gradient pruning and differential privacy require additional operations at every training epoch, whereas *Tazza* performs only a single shuffling operation once training is complete.

In Figure 15, we focus on the latency of operations in each scheme, excluding the time spent on model training to isolate the overhead introduced specifically for confidentiality attack mitigation. This experiment, conducted on a Raspberry Pi 3B, evaluates various model architectures to account for differences in computational overhead across models. The results in Figure 15 show that *Tazza* achieves the most efficient performance, primarily due to its reliance on a single shuffling operation after training completes, minimizing additional computational overhead.

Figure 16 depicts the latency of various defense schemes operating on different embedded platforms using an MLP model with a single hidden layer and 10 mini-batch updates. Overall, we can observe that *Tazza* shows superior performance compared to alternative mitigation approaches, by *Tazza* achieving up to 6.70 $\times$  lower latency compared to gradient pruning on the Raspberry Pi 3B. Furthermore, as a positive side-effect, Figure 16 shows that *Tazza* effectively reduces computational disparities among heterogeneous client platforms, with a 2.01 $\times$  difference in latency between the most powerful and weakest devices, compared to 2.68 $\times$  for gradient pruning. These results serve as evidence that *Tazza* is suitable for mobile/embedded federated learning systems.

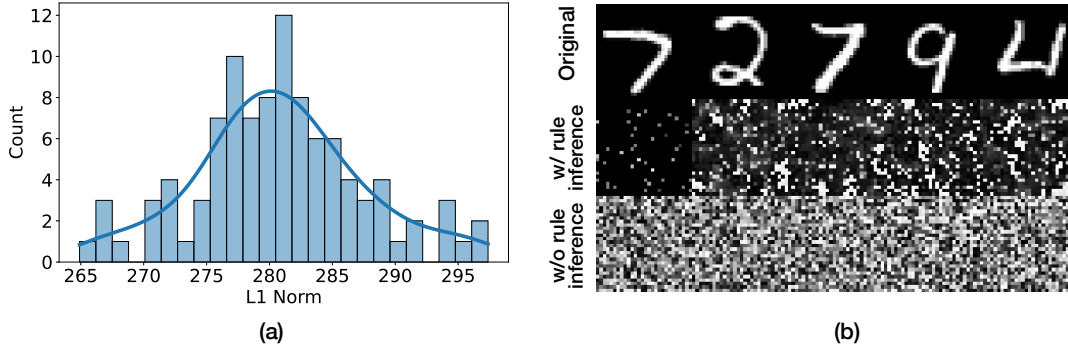


Fig. 17. (a) Average Error (L1-norm) between server inferred and the authentic shuffling order. (b) Confidentiality attack results showing the bottom-5 LPIPS values with and without the inference of the shuffling rule.

## 7.6 Impact of Adaptive Attacks

In this section, we demonstrate the robustness of *Tazza* against potential adaptive attacks, where an attacker possesses knowledge of the system and attempts to exploit it to bypass the defense mechanism.

**7.6.1 Parameter-based shuffling rule inference.** A key point to assure that *Tazza* operates as intended is to ensure the confidentiality of the shuffling rules from the server. However, it is practical to assume that the server would attempt counterattacks to infer this information. For instance, the server might try to deduce shuffling rules through neural network parameter analysis. As an initial study, we evaluate *Tazza*'s robustness against such attacks using an advanced adversary employing additional shuffling rule inference techniques. In this scenario, the attacker tries to identify a shuffling rule that minimizes the difference of the parameters (i.e., L2-norm) between the shuffled model parameters from the client against the global model.

To examine this, we used the MNIST dataset with 3-layered MLP models trained over a single update. Shuffling was applied only to the input layer, while the order of other layers remained unchanged, representing the simplest and most vulnerable configuration within our setup. Figure 17 (a) plots the distribution of average errors (L1-norm) between the inferred and ground truth shuffling rules across 100 clients. Note that we use the L1-norm since the shuffling rule can be interpreted as the indices of a given matrix. As the plots show, the average error was concentrated near 280, indicating that the index of a given row was located 280 rows off on average. This demonstrates the robustness of *Tazza* against a shuffling rule inference attack issued at the server. Figure 17 (b) visualizes the original samples that exhibited bottom-5 LPIPS values (5 most similar attack results) and the inferred samples via an inverting gradient attack with and without the shuffling rule inference. As the figure shows, the inferred samples are semantically uninterpretable, demonstrating the robustness of *Tazza* to adaptive attacks that try to infer the shuffling rule based on model parameters.

**7.6.2 Jigsaw puzzle-based shuffling rule inference.** In addition to rule inference using the parameters, there have also been efforts to train models capable of solving jigsaw puzzles to reconstruct original inputs from shuffled data [36]. While these studies have shown success in recovering shuffled data with a relatively small number of patches (e.g.,  $3 \times 3$ ), research on handling a large number of patches commonly used in neural networks (e.g.,  $14 \times 14$ ,  $16 \times 16$ ,  $32 \times 32$ ) and pixel-level shuffling remains mostly unexplored [10].

To evaluate the robustness of *Tazza* against such adaptive attacks, we conduct stress tests using the STL dataset and a transformer-based jigsaw puzzle solver [13]. Since these models are designed for high-resolution images ( $> 350 \times 350$ ) with a small number of patches (e.g.,  $3 \times 3$ ), we adopt the same configuration for this experiment.

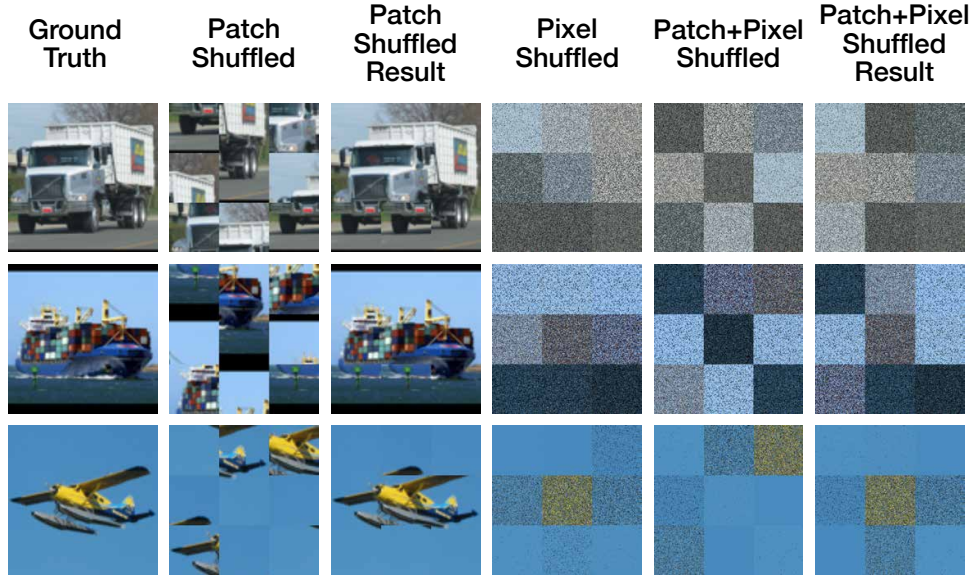


Fig. 18. Results of the jigsaw puzzle solver-based image restoration attack.

Figure 18 presents the results of image restoration attacks using the jigsaw puzzle solver. As the figure shows, the attack model successfully reconstructs certain aspects of the original images (‘Patch Shuffled Result’ in Figure 18). However, when both patch- and pixel-level shuffling are applied simultaneously, the model fails to recover the correct patch locations (‘Patch+Pixel Shuffled Result’ in Figure 18). Moreover, the semantic information becomes unrecognizable due to intra-patch pixel shuffling, which indicates *Tazza*’s resilience against such attacks.

Furthermore, even under relatively simple configurations, such as the MNIST dataset, the number of possible shuffling rules grows factorially (e.g.,  $(28 \times 28)! > 10^{1930}$ ), making it impractical for an attacker to recover the correct rule. For real-world datasets with high dimensional inputs, the search space of the shuffling rule expands exponentially, significantly increasing both the computational burden and infeasibility of launching a successful attack.

## 8 DISCUSSION

- Permutation Variant Neural Networks.** This work proposes *Tazza*, a framework addressing two core security challenges in federated learning by leveraging the permutation equivariance and invariance properties of neural networks. While these properties are commonly observed in modern neural networks, certain architectures (e.g., CNN) that lack these properties still persist [5]. While they can often be replaced with alternatives that exhibit these properties, there are cases where the model best suited for a specific application does not qualify these criteria. As a result, these models cannot directly leverage the weight shuffling mechanism in *Tazza*. However, it is important to note that many of these neural networks are optimized at the software level and are eventually transformed into matrix multiplication operations [12, 60]. Considering such optimization, it is feasible to devise new shuffling strategies tailored to these specific models, enabling their integration into the *Tazza* framework.

- Adaptive Attacks Against *Tazza*.** While we conducted an evaluation on two types of adaptive attacks, there remain potential adaptive strategies that malicious attackers could employ. For instance, attackers might use tampered shuffling rules before uploading their model to the server or leak the shuffling rule to the server. In the

case of attackers exploiting tampered shuffling rules, the tampered model is unlikely to impact benign clients, as the clustering algorithms employed by the server can effectively filter out such malicious models. Additionally, the server can enhance the integrity of the federated learning pipeline by incorporating a zero-knowledge proof (ZKP) approach to verify that the shuffled weights have not been tampered with.

In the (unlikely) case where the shuffling rule is leaked, clients can implement additional security measures, such as secure multi-party computation (SMPC), during the rule-sharing process. This ensures that each client holds only partial information about the shuffling rule, thereby preventing attackers from gaining full knowledge of the rule without the cooperation of benign clients. While these approaches are promising and effective, they introduce additional computational and communication overhead. Consequently, designing efficient and effective security protocols or features represents an important and compelling direction for future research.

• **Network Scalability.** From a systems perspective, a critical consideration for *Tazza* is its scalability. *Tazza* relies on secure peer-to-peer communication for exchanging shuffling rules. In scenarios where geographically dispersed clients are selected, clients have limited communication capabilities, or the number of clients becomes very large, thus the communication stability and computational or time cost of communication may pose challenges. However, rather than directly sharing full shuffling matrices, a more lightweight approach, such as exchanging random seeds, can significantly reduce the overhead. Nevertheless, a deeper analysis on scalability remains a valuable direction for future work, particularly to address potential bottlenecks and ensure the system’s robustness in more demanding settings.

## 9 CONCLUSION

In this paper, we introduce *Tazza*, a secure, privacy-preserving, and efficient federated learning framework designed to address the intertwined challenges of integrity and confidentiality in decentralized systems. Leveraging the permutation equivariance and invariance properties inherent in modern neural networks, *Tazza* employs innovative components such as Weight Shuffling and Shuffled Model Validation to enhance resilience against a wide range of attacks, including model poisoning and data leakage. Comprehensive evaluations across diverse datasets and embedded computing platforms demonstrate that *Tazza* effectively mitigates both integrity and confidentiality threats while maintaining high model accuracy and achieving up to 6.7× computational efficiency compared to alternative defense schemes. These results highlight the potential of *Tazza* as a practical and robust solution for secure federated learning in real-world scenarios, catalyzing future research in balancing privacy, security, and performance in decentralized systems.

## REFERENCES

- [1] Martin Abadi, Andy Chu, Ian Goodfellow, H Brendan McMahan, Ilya Mironov, Kunal Talwar, and Li Zhang. 2016. Deep learning with differential privacy. In *Proceedings of the 2016 ACM SIGSAC conference on computer and communications security*. 308–318.
- [2] Samiul Alam, Tuo Zhang, Tiantian Feng, Hui Shen, Zhichao Cao, Dong Zhao, JeongGil Ko, Kiran Somasundaram, Shrikanth S Narayanan, Salman Avestimehr, et al. 2023. FedAIoT: A Federated Learning Benchmark for Artificial Intelligence of Things. *arXiv preprint arXiv:2310.00109* (2023).
- [3] Al Amin, Kamrul Hasan, Sharif Ullah, and M Shamim Hossain. 2024. ViT Enhanced Privacy-Preserving Secure Medical Data Sharing and Classification. *arXiv preprint arXiv:2411.05901* (2024).
- [4] Eugene Bagdasaryan, Andreas Veit, Yiqing Hua, Deborah Estrin, and Vitaly Shmatikov. 2020. How to backdoor federated learning. In *International conference on artificial intelligence and statistics*. PMLR, 2938–2948.
- [5] Peter W Battaglia, Jessica B Hamrick, Victor Bapst, Alvaro Sanchez-Gonzalez, Vinicius Zambaldi, Mateusz Malinowski, Andrea Tacchetti, David Raposo, Adam Santoro, Ryan Faulkner, et al. 2018. Relational inductive biases, deep learning, and graph networks. *arXiv preprint arXiv:1806.01261* (2018).
- [6] Battista Biggio, Blaine Nelson, and Pavel Laskov. 2012. Poisoning attacks against support vector machines. *arXiv preprint arXiv:1206.6389* (2012).
- [7] Peva Blanchard, El Mahdi El Mhamdi, Rachid Guerraoui, and Julien Stainer. 2017. Machine learning with adversaries: Byzantine tolerant gradient descent. *Advances in neural information processing systems* 30 (2017).

- [8] EunSeong Boo, Joongheon Kim, and JeongGil Ko. 2021. LiteZKP: Lightening zero-knowledge proof-based blockchains for IoT and edge platforms. *IEEE Systems Journal* 16, 1 (2021), 112–123.
- [9] Xiaoyu Cao, Minghong Fang, Jia Liu, and Neil Zhenqiang Gong. 2020. Fltrust: Byzantine-robust federated learning via trust bootstrapping. *arXiv preprint arXiv:2012.13995* (2020).
- [10] Fabio M Carlucci, Antonio D’Innocente, Silvia Bucci, Barbara Caputo, and Tatiana Tommasi. 2019. Domain generalization by solving jigsaw puzzles. In *Proceedings of the IEEE/CVF conference on computer vision and pattern recognition*. 2229–2238.
- [11] Miguel Castro, Barbara Liskov, et al. 1999. Practical byzantine fault tolerance. In *OsDI*, Vol. 99. 173–186.
- [12] Kumar Chellapilla, Sidd Puri, and Patrice Simard. 2006. High performance convolutional neural networks for document processing. In *Tenth international workshop on frontiers in handwriting recognition*. Suvisoft.
- [13] Yingyi Chen, Xi Shen, Yahui Liu, Qinghua Tao, and Johan A. K. Suykens. 2023. Jigsaw-ViT: Learning Jigsaw Puzzles in Vision Transformer. *Pattern Recognition Letters* 166 (2023), 53–60.
- [14] Adam Coates, Andrew Ng, and Honglak Lee. 2011. An analysis of single-layer networks in unsupervised feature learning. In *Proceedings of the fourteenth international conference on artificial intelligence and statistics*. JMLR Workshop and Conference Proceedings, 215–223.
- [15] Li Deng. 2012. The mnist database of handwritten digit images for machine learning research. *IEEE Signal Processing Magazine* 29, 6 (2012), 141–142.
- [16] Alexey Dosovitskiy, Lucas Beyer, Alexander Kolesnikov, Dirk Weissenborn, Xiaohua Zhai, Thomas Unterthiner, Mostafa Dehghani, Matthias Minderer, Georg Heigold, Sylvain Gelly, et al. 2020. An image is worth 16x16 words: Transformers for image recognition at scale. *arXiv preprint arXiv:2010.11929* (2020).
- [17] Cynthia Dwork, Aaron Roth, et al. 2014. The algorithmic foundations of differential privacy. *Foundations and Trends® in Theoretical Computer Science* 9, 3–4 (2014), 211–407.
- [18] Fatima Elhattab, Sara Bouchenak, and Cédric Boscher. 2024. Pastel: Privacy-preserving federated learning in edge computing. *Proceedings of the ACM on Interactive, Mobile, Wearable and Ubiquitous Technologies* 7, 4 (2024), 1–29.
- [19] Fatima Elhattab, Sara Bouchenak, Rania Talbi, and Vlad Nitu. 2023. Robust federated learning for ubiquitous computing through mitigation of edge-case backdoor attacks. *Proceedings of the ACM on Interactive, Mobile, Wearable and Ubiquitous Technologies* 6, 4 (2023), 1–27.
- [20] Martin Ester, Hans-Peter Kriegel, Jörg Sander, Xiaowei Xu, et al. 1996. A density-based algorithm for discovering clusters in large spatial databases with noise. In *kdd*, Vol. 96. 226–231.
- [21] Minghong Fang, Xiaoyu Cao, Jinyuan Jia, and Neil Gong. 2020. Local model poisoning attacks to {Byzantine-Robust} federated learning. In *29th USENIX security symposium (USENIX Security 20)*. 1605–1622.
- [22] Jie Feng, Can Rong, Funing Sun, Diansheng Guo, and Yong Li. 2020. PMF: A privacy-preserving human mobility prediction framework via federated learning. *Proceedings of the ACM on Interactive, Mobile, Wearable and Ubiquitous Technologies* 4, 1 (2020), 1–21.
- [23] Yongjian Fu, Lanqing Yang, Hao Pan, Yi-Chao Chen, Guangtao Xue, and Ju Ren. 2024. MagSpy: Revealing User Privacy Leakage via Magnetometer on Mobile Devices. *IEEE Transactions on Mobile Computing* (2024).
- [24] Clement Fung, Chris JM Yoon, and Ivan Beschastnikh. 2020. The limitations of federated learning in sybil settings. In *23rd International Symposium on Research in Attacks, Intrusions and Defenses (RAID 2020)*. 301–316.
- [25] Jonas Geiping, Hartmut Bauermeister, Hannah Dröge, and Michael Moeller. 2020. Inverting gradients-how easy is it to break privacy in federated learning? *Advances in Neural Information Processing Systems* 33 (2020), 16937–16947.
- [26] Tzu-Ming Harry Hsu, Hang Qi, and Matthew Brown. 2019. Measuring the effects of non-identical data distribution for federated visual classification. *arXiv preprint arXiv:1909.06335* (2019).
- [27] Yangsibo Huang, Samyak Gupta, Zhao Song, Kai Li, and Sanjeev Arora. 2021. Evaluating gradient inversion attacks and defenses in federated learning. *Advances in neural information processing systems* 34 (2021), 7232–7241.
- [28] Ehsanul Kabir, Zeyu Song, Md Rafi Ur Rashid, and Shagufta Mehnaz. 2024. Flshield: a validation based federated learning framework to defend against poisoning attacks. In *2024 IEEE Symposium on Security and Privacy (SP)*. IEEE, 2572–2590.
- [29] Hyunjun Kim and JeongGil Ko. 2022. Fast Monte-Carlo approximation of the attention mechanism. In *Proceedings of the AAAI conference on artificial intelligence*, Vol. 36. 7185–7193.
- [30] Diederik P Kingma and Jimmy Ba. 2014. Adam: A method for stochastic optimization. *arXiv preprint arXiv:1412.6980* (2014).
- [31] Alex Krizhevsky, Geoffrey Hinton, et al. 2009. Learning multiple layers of features from tiny images. (2009).
- [32] Kichang Lee, Yujin Shin, Jonghyuk Yun, Jun Han, and JeongGil Ko. 2024. DeTrigger: A Gradient-Centric Approach to Backdoor Attack Mitigation in Federated Learning. *arXiv preprint arXiv:2411.12220* (2024).
- [33] Kichang Lee, Jonghyuk Yun, Jun Han, and Jeonggil Ko. 2023. Exploiting Indices for Man-in-the-Middle Attacks on Collaborative Unpooling Autoencoders. In *Proceedings of the 21st Annual International Conference on Mobile Systems, Applications and Services*. 598–599.
- [34] Kichang Lee, Jonghyuk Yun, Jaeho Jin, Jun Han, and JeongGil Ko. 2025. Mind your indices! Index hijacking attacks on collaborative unpooling autoencoder systems. *Internet of Things* 29 (2025), 101462.
- [35] Sungmin Lee, Kichang Lee, JaeYeon Park, and JeongGil Ko. 2024. GMT: Gzip-based Memory-efficient Time-series classification. *ICT Express* (2024).

- [36] Ru Li, Shuaicheng Liu, Guangfu Wang, Guanghui Liu, and Bing Zeng. 2021. Jigsawgan: Auxiliary learning for solving jigsaw puzzles with generative adversarial networks. *IEEE Transactions on Image Processing* 31 (2021), 513–524.
- [37] Bingyan Liu, Yifeng Cai, Ziqi Zhang, Yuanchun Li, Leye Wang, Ding Li, Yao Guo, and Xiangqun Chen. 2021. Distfl: Distribution-aware federated learning for mobile scenarios. *Proceedings of the ACM on Interactive, Mobile, Wearable and Ubiquitous Technologies* 5, 4 (2021), 1–26.
- [38] Brendan McMahan, Eider Moore, Daniel Ramage, Seth Hampson, and Blaise Aguera y Arcas. 2017. Communication-efficient learning of deep networks from decentralized data. In *Artificial intelligence and statistics*. PMLR, 1273–1282.
- [39] Fan Mo, Hamed Haddadi, Kleomenis Katevas, Eduard Marin, Diego Perino, and Nicolas Kourtellis. 2021. PPFL: Privacy-preserving federated learning with trusted execution environments. In *Proceedings of the 19th annual international conference on mobile systems, applications, and services*. 94–108.
- [40] George B Moody and Roger G Mark. 1992. MIT-BIH arrhythmia database. (*No Title*) (1992).
- [41] George B Moody and Roger G Mark. 2001. The impact of the MIT-BIH arrhythmia database. *IEEE engineering in medicine and biology magazine* 20, 3 (2001), 45–50.
- [42] Muhammad Muzammal Naseer, Kanchana Ranasinghe, Salman H Khan, Munawar Hayat, Fahad Shahbaz Khan, and Ming-Hsuan Yang. 2021. Intriguing properties of vision transformers. *Advances in Neural Information Processing Systems* 34 (2021), 23296–23308.
- [43] Nvidia. 2019. Nvidia Jetson Nano Developer Kit. <https://shorturl.at/u03A0>.
- [44] Nvidia. 2019. Nvidia Jetson TX2 Developer Kit. <https://shorturl.at/QENkj>.
- [45] Xiaomin Ouyang, Xian Shuai, Yang Li, Li Pan, Xifan Zhang, Heming Fu, Sitong Cheng, Xinyan Wang, Shihua Cao, Jiang Xin, et al. 2024. ADMarker: A Multi-Modal Federated Learning System for Monitoring Digital Biomarkers of Alzheimer’s Disease. In *Proceedings of the 30th Annual International Conference on Mobile Computing and Networking*. 404–419.
- [46] HyeonJung Park, Youngki Lee, and JeongGil Ko. 2021. Enabling Real-Time Sign Language Translation on Mobile Platforms with On-Board Depth Cameras. *Proc. ACM Interact. Mob. Wearable Ubiquitous Technol.* 5, 2, Article 77 (jun 2021), 30 pages.
- [47] Jaeyeon Park, Hyeon Cho, Rajesh Krishna Balan, and JeongGil Ko. 2020. Heartquake: Accurate low-cost non-invasive ecg monitoring using bed-mounted geophones. *Proceedings of the ACM on Interactive, Mobile, Wearable and Ubiquitous Technologies* 4, 3 (2020), 1–28.
- [48] JaeYeon Park, Kichang Lee, Sungmin Lee, Mi Zhang, and JeongGil Ko. 2023. AttFL: A Personalized Federated Learning Framework for Time-series Mobile and Embedded Sensor Data Processing. *Proceedings of the ACM on Interactive, Mobile, Wearable and Ubiquitous Technologies* 7, 3 (2023), 1–31.
- [49] JaeYeon Park, Kichang Lee, Noseong Park, Seng Chan You, and JeongGil Ko. 2023. Self-Attention LSTM-FCN model for arrhythmia classification and uncertainty assessment. *Artificial Intelligence in Medicine* 142 (2023), 102570.
- [50] Adam Paszke, Sam Gross, Francisco Massa, Adam Lerer, James Bradbury, Gregory Chanan, Trevor Killeen, Zeming Lin, Natalia Gimelshein, Luca Antiga, et al. 2019. Pytorch: An imperative style, high-performance deep learning library. *Advances in neural information processing systems* 32 (2019).
- [51] L Perez. 2017. The effectiveness of data augmentation in image classification using deep learning. *arXiv preprint arXiv:1712.04621* (2017).
- [52] Raspberry Pi. 2023. [shorturl.at](https://shorturl.at/U4bVU). <https://shorturl.at/U4bVU>.
- [53] Frank Rosenblatt. 1958. The perceptron: a probabilistic model for information storage and organization in the brain. *Psychological review* 65, 6 (1958), 386.
- [54] David E Rumelhart, Geoffrey E Hinton, and Ronald J Williams. 1986. Learning representations by back-propagating errors. *nature* 323, 6088 (1986), 533–536.
- [55] Lorenzo Sani, Alex Iacob, Zeyu Cao, Royson Lee, Bill Marino, Yan Gao, Dongqi Cai, Zexi Li, Wanru Zhao, Xinchu Qiu, et al. 2024. Photon: Federated LLM Pre-Training. *arXiv preprint arXiv:2411.02908* (2024).
- [56] Yujin Shin, Kichang Lee, Sungmin Lee, You Rim Choi, Hyung-Sin Kim, and JeongGil Ko. 2024. Effective Heterogeneous Federated Learning via Efficient Hypernetwork-based Weight Generation. In *Proceedings of the 22nd ACM Conference on Embedded Networked Sensor Systems*. 112–125.
- [57] Connor Shorten and Taghi M Khoshgoftaar. 2019. A survey on image data augmentation for deep learning. *Journal of big data* 6, 1 (2019), 1–48.
- [58] Ke Sun, Chen Chen, and Xinyu Zhang. 2020. " Alexa, stop spying on me!" speech privacy protection against voice assistants. In *Proceedings of the 18th conference on embedded networked sensor systems*. 298–311.
- [59] Ilya O Tolstikhin, Neil Houlsby, Alexander Kolesnikov, Lucas Beyer, Xiaohua Zhai, Thomas Unterthiner, Jessica Yung, Andreas Steiner, Daniel Keysers, Jakob Uszkoreit, et al. 2021. Mlp-mixer: An all-mlp architecture for vision. *Advances in neural information processing systems* 34 (2021), 24261–24272.
- [60] Aravind Vasudevan, Andrew Anderson, and David Gregg. 2017. Parallel multi channel convolution using general matrix multiplication. In *2017 IEEE 28th international conference on application-specific systems, architectures and processors (ASAP)*. IEEE, 19–24.
- [61] Xiaohua Wu, Hongji Ling, Huan Liu, and Fangjian Yu. 2022. A privacy-preserving and efficient byzantine consensus through multi-signature with ring. *Peer-to-Peer Networking and Applications* 15, 3 (2022), 1669–1684.
- [62] Cong Xie, Oluwasanmi Koyejo, and Indranil Gupta. 2018. Generalized byzantine-tolerant sgd. *arXiv preprint arXiv:1802.10116* (2018).

- [63] Zhiyuan Xie, Xiaomin Ouyang, Li Pan, Wenrui Lu, Guoliang Xing, and Xiaoming Liu. 2023. Mozart: A Mobile ToF System for Sensing in the Dark through Phase Manipulation. In *Proceedings of the 21st Annual International Conference on Mobile Systems, Applications and Services*. 163–176.
- [64] Hengyuan Xu, Liyao Xiang, Hangyu Ye, Dixi Yao, Pengzhi Chu, and Baochun Li. 2024. Permutation Equivariance of Transformers and Its Applications. In *Proceedings of the IEEE/CVF Conference on Computer Vision and Pattern Recognition*. 5987–5996.
- [65] Dong Yin, Yudong Chen, Ramchandran Kannan, and Peter Bartlett. 2018. Byzantine-robust distributed learning: Towards optimal statistical rates. In *International conference on machine learning*. Pmlr, 5650–5659.
- [66] Jonghyuk Yun, Kyoosik Lee, Kichang Lee, Bangjie Sun, Jaeho Jeon, Jeonggil Ko, Inseok Hwang, and Jun Han. 2024. PowDew: Detecting Counterfeit Powdered Food Products using a Commodity Smartphone. In *Proceedings of the 22nd Annual International Conference on Mobile Systems, Applications and Services*. 210–222.
- [67] Huaqing Zhang, Xiaolin Cheng, Hui Zang, and Dae Hoon Park. 2019. Compiler-level matrix multiplication optimization for deep learning. *arXiv preprint arXiv:1909.10616* (2019).
- [68] Richard Zhang, Phillip Isola, Alexei A Efros, Eli Shechtman, and Oliver Wang. 2018. The unreasonable effectiveness of deep features as a perceptual metric. In *Proceedings of the IEEE conference on computer vision and pattern recognition*. 586–595.
- [69] Chuan Zhao, Shengnan Zhao, Minghao Zhao, Zhenxiang Chen, Chong-Zhi Gao, Hongwei Li, and Yu-an Tan. 2019. Secure multi-party computation: theory, practice and applications. *Information Sciences* 476 (2019), 357–372.
- [70] Ligeng Zhu, Zhijian Liu, and Song Han. 2019. Deep leakage from gradients. *Advances in neural information processing systems* 32 (2019).